

# Advanced Porous Materials as Designer Platforms for Sequestering Radionuclide Pertechnetate

Published as part of *Chem & Bio Engineering* virtual special issue “Advanced Separation Materials and Processes”.

Zhiwei Xing,<sup>¶</sup> Zhuozhi Lai,<sup>¶</sup> Qi Sun,\* Chengliang Xiao, Shuao Wang, Xiangke Wang, Briana Aguila-Ames, Praveen K. Thallapally, Kyle Martin, and Shengqian Ma\*



Cite This: *Chem Bio Eng.* 2024, 1, 199–222



Read Online

ACCESS |



Metrics & More



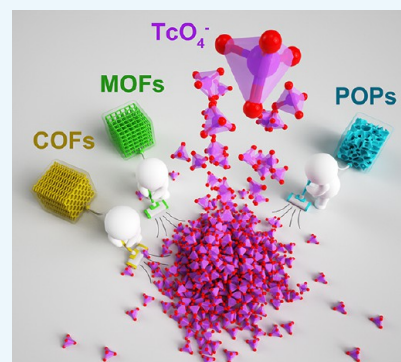
Article Recommendations



Supporting Information

**ABSTRACT:** Technetium-99 ( $^{99}\text{Tc}$ ), predominantly present as pertechnetate ( $^{99}\text{TcO}_4^-$ ), is a challenging contaminant in nuclear waste from artificial nuclear fission. The selective removal of  $^{99}\text{TcO}_4^-$  from nuclear waste and contaminated groundwater is complex due to (i) the acidic and intricate nature of high-level liquid wastes; (ii) the highly alkaline environment in low-activity level tank wastes, such as those at Hanford, and in high-level wastes at locations like Savannah River; and (iii) the potential for  $^{99}\text{TcO}_4^-$  to leak into groundwater, risking severe water pollution due to its high mobility. This Review focuses on recent developments in advanced porous materials, including metal–organic frameworks (MOFs), covalent organic frameworks (COFs), and their amorphous counterparts, porous organic polymers (POPs). These materials have demonstrated exceptional effectiveness in adsorbing  $^{99}\text{TcO}_4^-$  and similar oxyanions. We comprehensively review the adsorption mechanisms of these anions with the adsorbents, employing macroscopic batch/column experiments, microscopic spectroscopic analyses, and theoretical calculations. In conclusion, we present our perspectives on potential future research directions, aiming to overcome current challenges and explore new opportunities in this area. Our goal is to encourage further research into the development of advanced porous materials for efficient  $^{99}\text{TcO}_4^-$  management.

**KEYWORDS:** nuclear waste treatment,  $^{99}\text{TcO}_4^-$  removal, metal–organic frameworks, covalent organic frameworks, organic polymers



## INTRODUCTION

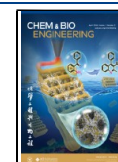
As exacerbating global energy crisis and mounting concerns over the greenhouse effect seize the world's attention, it has become critically important to fundamentally rethink how we use and source energy. The urgent need for carbon reduction and the push toward carbon neutrality are now major global issues that demand robust solutions. As an avenue worth exploring in our quest to address these challenges, nuclear power, noted for its negligible emissions of  $\text{CO}_2$ ,  $\text{NO}_x$ , and  $\text{SO}_2$ , presents an intriguing possibility.<sup>1–4</sup> In the greater picture of global energy production, nuclear energy holds a crucial place. The report published by the International Atomic Energy Agency, titled “International Status and Prospects for Nuclear Power 2021,” discloses that by the close of 2020, the world was powered by 441 operational nuclear power units. Together, this vast network denoted a total installed power capacity of close to 392 gigawatt-electric (GWe), contributing to around 15% of the world's total power generation.<sup>5–7</sup> Moreover, these power plants create approximately 10,000 tons of spent nuclear fuel each year. However, along with the opportunities nuclear energy presents, there also exist numerous environmental and safety concerns necessitating our attention. In the lifecycle of nuclear energy

production, the release of radionuclides occurs at several stages, including the mining and processing of uranium, the operational phase of nuclear power plants, and the management of spent nuclear fuel. These stages figure elemental notables such as  $^{235}\text{U}$  or  $^{238}\text{U}$ ,  $^{131}\text{I}$ ,  $^3\text{H}$ ,  $^{14}\text{C}$ ,  $^{85}\text{Kr}$ ,  $^{90}\text{Sr}$ ,  $^{137}\text{Cs}$ , and  $^{235}\text{U}$ ,  $^{99}\text{Tc}$ ,  $^{239,240}\text{Pu}$ ,  $^{237}\text{Np}$ , respectively.<sup>8,9</sup> Radionuclides are also unconsciously released into the environment during nuclear tests and facility operations. These elements, due to their radioactive toxicity, solubility, and mobility along with their  $\alpha$ ,  $\beta$ , and  $\gamma$  irradiation, pose a substantial risk factor. If allowed to contaminate our food chain and subsequent ingestion, these substances could cause grievous harm. Their danger is especially pronounced in ecosystems intervened by radionuclides with long half-lives. Hence, the issue of nuclear security surfaces as a pressing, global

**Received:** December 28, 2023

**Accepted:** February 19, 2024

**Published:** February 22, 2024



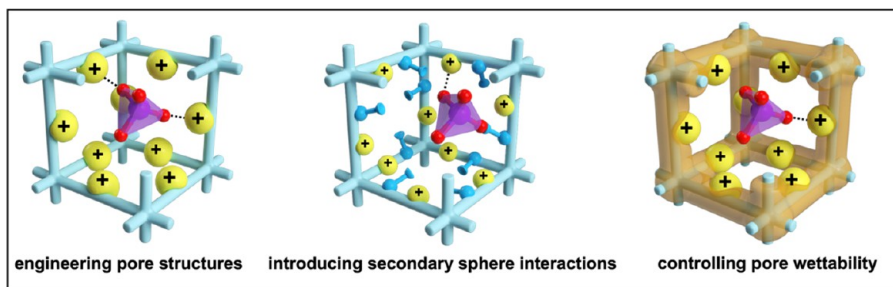


**Figure 1.** Strategies for enhancing the segregation efficiency of  $\text{TcO}_4^-$ : (a) engineering pore structures to increase charge density, (b) introducing secondary sphere interactions to strengthen binding, and (c) controlling pore wettability to improve binding affinity.

challenge that demands our immediate attention, specifically toward the safe and secure operation of nuclear power plants and the responsible management of nuclear waste. The sustainable advancement of nuclear energy necessitates a keen focus on the effective treatment and disposal of used nuclear fuel and the management of legacy nuclear waste.<sup>10–12</sup> Successfully tackling these challenges is crucial for leveraging the advantages of nuclear power while minimizing its environmental and health repercussions.

A significant hurdle in the nuclear fuel cycle is presented by  $^{99}\text{Tc}$ . This isotope is characterized by a notably long half-life of 213,000 years and its  $\beta$ -emission properties.<sup>13–16</sup>  $^{99}\text{Tc}$  is produced in considerable amounts as a byproduct of used nuclear fuel, with an impressive fission yield of 6.05%. To put this into perspective, a nuclear reactor with a 1 GWe capacity produces about 21 kg of  $^{99}\text{Tc}$  each year. Since the dawn of nuclear power, this has culminated in a global total of approximately 400 metric tonnes of  $^{99}\text{Tc}$ .<sup>17–21</sup> The primary form of  $^{99}\text{Tc}$  in the environment is pertechnetate ( $\text{TcO}_4^-$ ), an anion known for its high solubility and poor ability to form complexes.<sup>22,23</sup> These properties allow it to move swiftly through various environments, bypassing minerals and organic substances with ease. Such mobility poses substantial concerns regarding the contamination of groundwater and the potential risks to aquatic ecosystems, especially in locations with legacy radioactive waste from historical power production and military activities. A prominent illustration of the complexities inherent in nuclear waste management is exemplified by the Hanford Site in Washington State. At this location, millions of gallons of mixed hazardous and radioactive wastes are stored, representing one of the most extensive environmental cleanup endeavors globally. The imperative to ensure the effective containment and appropriate management of nuclear waste until it undergoes processing in a waste treatment and immobilization plant is paramount for addressing the enduring challenge of nuclear waste and concurrently mitigating its environmental impact. Within the domain of used nuclear fuel processing, particularly in the plutonium–uranium redox extraction (PUREX) process, the element  $^{99}\text{Tc}$  presents a significant challenge.<sup>24,25</sup> Its propensity to co-extract with key fissile materials such as uranium, neptunium, and plutonium complicates their purification. Moreover, the volatility of  $^{99}\text{Tc}$  compounds introduces a substantial risk of escape, especially during the vitrification process of nuclear waste. Effectively addressing this issue by removing  $^{99}\text{Tc}$  early in the PUREX process would be highly advantageous, enhancing risk management and streamlining nuclear waste treatment. However, the extraction of  $\text{TcO}_4^-$  from spent nuclear fuels encounters formidable challenges, primarily attributed to the harsh conditions inherent in nuclear waste

environments. This setting is marked by extreme acidity, with a concentration of 3 M  $\text{HNO}_3$ . Additionally, the presence of a multitude of metal and nonmetal ions imparts a high ionic strength, further complicating the separation process. Furthermore, the surroundings are characterized by a formidable radiation field, encompassing  $\beta$ ,  $\gamma$ , and neutron radiation. Another facet of the challenge is evident in dealing with legacy tank waste at the Savannah River Site (SRS), where highly active  $\text{TcO}_4^-$  is dissolved in solutions characterized by both high alkalinity and brine-like properties.<sup>26</sup> Managing such hazardous and complex waste necessitates innovative and robust solutions, as it involves handling some of the most corrosive and radioactive materials known. The development of effective methods to isolate and manage  $^{99}\text{Tc}$  in these diverse and demanding environments is therefore crucial for advancing nuclear waste treatment technologies and ensuring environmental safety.

The management of nuclear waste streams, particularly the removal of the predominant  $^{99}\text{Tc}$  species as  $\text{TcO}_4^-$ , has led to the exploration of various anion-exchanging materials. The radioactivity of the  $^{99}\text{Tc}$  isotope necessitates specialized handling procedures, often in nonstandard laboratory environments. Consequently,  $\text{ReO}_4^-$  is frequently used as a substitute for  $\text{TcO}_4^-$  in research because of their similar speciation, dimensions, hydration energies, and volatility (Table S1).<sup>27–29</sup> Several materials have been explored for their efficacy in extracting  $^{99}\text{Tc}$  from nuclear waste solutions. These include ion-exchange resins such as superLig-639 or Purolite-A-520E,<sup>30,31</sup> layered double hydroxides (LDH),<sup>32–36</sup> modified natural clays,<sup>37–39</sup> and graphene-based materials.<sup>40–42</sup> Despite these efforts, many of these adsorbents suffer from drawbacks such as slow anion-exchange kinetics, inadequate radiation resistance, or insufficient sorption capacity and selectivity. As a result, despite extensive research and development, the environmental challenges posed by  $^{99}\text{Tc}$  at legacy nuclear sites remain significant. However, there is growing optimism with the emergence of advanced porous materials, including metal–organic frameworks (MOFs),<sup>43–47</sup> covalent organic frameworks (COFs),<sup>48–52</sup> and their amorphous counterparts, porous organic polymers (POPs).<sup>53–55</sup> The primary benefit of these advanced materials is their adaptability, which enables exact modifications to their functionality. By manipulating their structure and composition at the atomic scale and comprehending the relationships between structure and properties, these porous materials can be tailored for a wide range of uses. This innovation presents promising opportunities to surpass the constraints of conventional materials in effectively and selectively extracting  $^{99}\text{Tc}$  from nuclear waste streams (Tables S2 and S3).

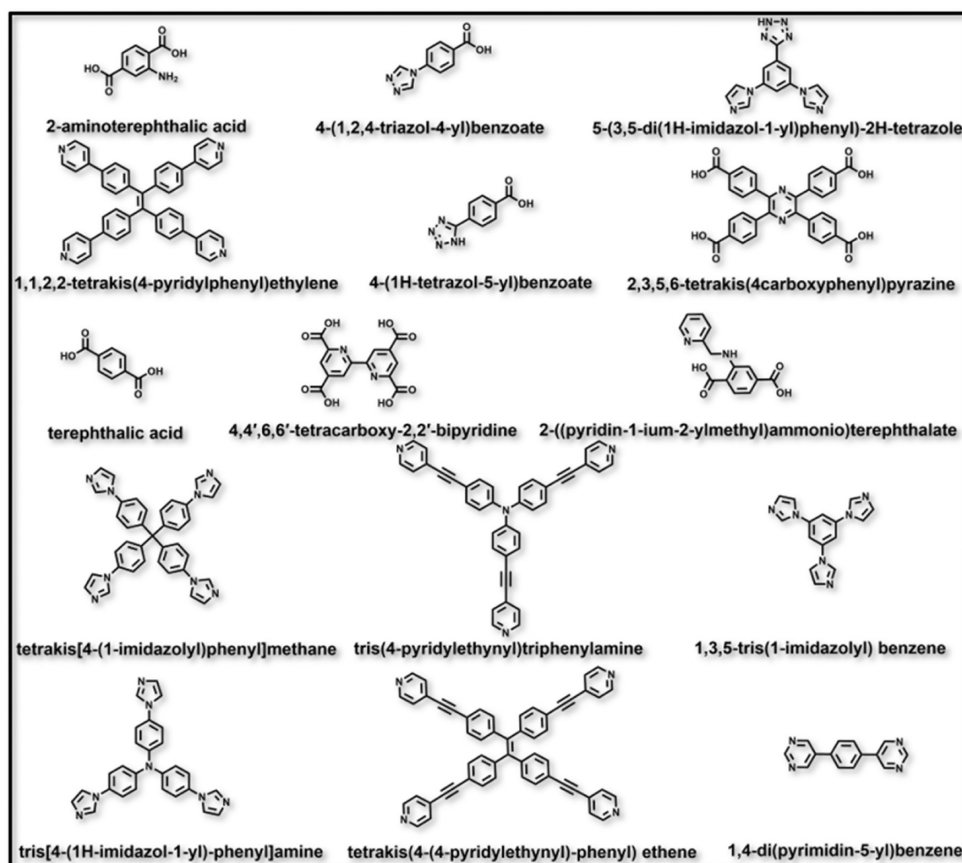


**Figure 2.** Molecular structures of organic ligands utilized in the construction of the MOFs discussed within this Review.

The synthetic strategy employed for targeting adsorbent materials, particularly in the context of  $\text{TcO}_4^-$  sequestration, exhibits remarkable efficacy by focusing on *de novo* synthesis. In this approach, each monomer undergoes meticulous crafting to accommodate distinct functional groups, thereby significantly enhancing the sequestration performance for the target analyte in terms of both uptake capacity and selectivity. This methodology represents a substantial advancement compared to traditional adsorbents that lack the tailored specificity inherent in these sophisticated materials. Although this approach may entail additional costs, the benefits derived from improved capacity and selectivity effectively outweigh these expenses. The customization of these materials extends beyond the integration of functional groups; it encompasses the engineering of pore structures to increase charge density, the introduction of secondary sphere interactions to strengthen binding, and the control of pore wettability to amplify sorption performance (Figure 1). The strategically designed channels within these materials serve as conduits for contaminants, while the proximity of functional groups heightens their interaction with the target analytes. This Review aims to comprehensively outline the latest research efforts in the development of advanced porous solids dedicated to  $\text{TcO}_4^-$  sequestration. It underscores the design strategies and underlying principles, emphasizing the distinctive attributes of these materials in selectively capturing contaminants. Through the synergy of customizable starting units and pore structures, combined with the inherent tunability of these materials, they can be effectively tailored to enhance  $\text{TcO}_4^-$  removal, showcasing their potential in addressing this environmental challenge. Additionally, this

Review delineates the persisting challenges in effectively removing  $\text{TcO}_4^-$  from complex environments, providing insight into areas requiring further exploration and innovation.

## MOF-BASED SORBENTS

MOFs are a class of framework materials characterized by their unique structure, where metal clusters are coordinated with organic ligands (the molecular structures of which are depicted in Figure 2), giving rise to one-, two-, or three-dimensional (1D, 2D, or 3D) porous structures. Their key advantage lies in the rigid topology of their node–strut arrangement and the nature of their coordination bonding. This structural blueprint allows for precise control over their composition and configuration, thereby leveraging potent noncovalent intermolecular interactions. In the realm of MOFs, Thallapally and colleagues pioneered the utilization of MOFs for eliminating  $\text{TcO}_4^-$ . Their approach involved the synthesis of a cationic MOF by modifying UiO-66- $\text{NH}_2$  in acidic conditions. This modification process converted the  $\mu\text{-OH}$  group into a  $[\mu\text{-OH}_2]^+$  moiety while also protonating the  $\text{-NH}_2$  group. These changes significantly enhanced the anion-exchange performance of UiO-66- $\text{NH}_2$ . The modified MOF demonstrated an uptake capacity for  $\text{ReO}_4^-$ , at  $159 \text{ mg g}^{-1}$ , outperforming traditional inorganic ion-exchange materials like LDHs. However, it showed limited selectivity in the presence of competing anions such as  $\text{PO}_4^{3-}$ ,  $\text{SO}_4^{2-}$ ,  $\text{ClO}_4^-$ , and  $\text{NO}_3^-$ , following an adsorption trend of  $\text{PO}_4^{3-} > \text{SO}_4^{2-} \approx \text{ClO}_4^- \approx \text{NO}_3^- \approx \text{ReO}_4^-$ .<sup>56</sup> In a parallel advancement, Hu and team synthesized CAU-1, an aluminum-based MOF, by reacting 2-aminoterephthalic acid with aluminum chloride. The presence of cationic protonated amines

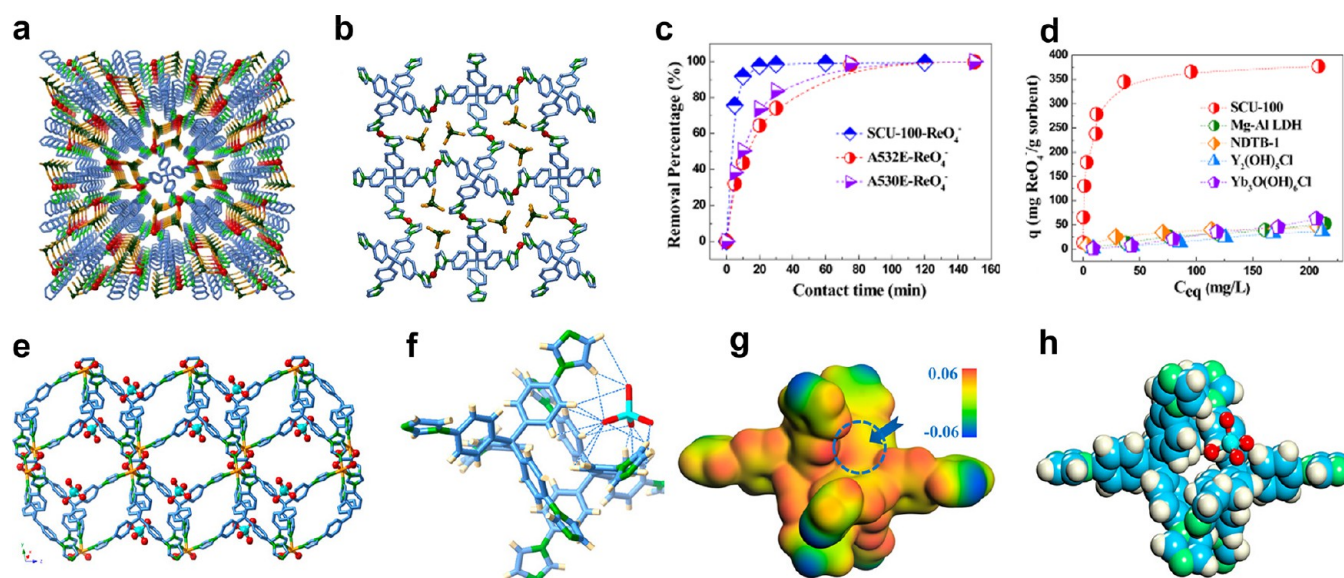


**Figure 3.** (a) Perspective packing structure of SCU-100-Re viewed along the  $c$  axis. (b) One single-network crystal structure depiction of SCU-100-Re. (c) Comparison of the sorption kinetics of  $\text{ReO}_4^-$  by SCU-100, A532E, and A530E. (d) Sorption isotherms of  $\text{ReO}_4^-$  by cationic SCU-100 compared with Mg-Al LDH, NDTB-1,  $\text{Y}_2(\text{OH})_3\text{Cl}$ , and  $\text{Yb}_3\text{O}(\text{OH})_6\text{Cl}$  materials. Panels a–d are reproduced from ref 58. Copyright 2017, American Chemical Society. (e)  $\text{TcO}_4^-$  trapped in type A channels. (f) Hydrogen bonds formed between  $\text{TcO}_4^-$  and SCU-101 framework. (g) Electrostatic potential distribution of the partial framework. (h) Optimized trapping position of  $\text{TcO}_4^-$  in the framework by theoretical calculations. Panels e–h are reproduced from ref 59. Copyright 2017, American Chemical Society.

( $\text{NH}_3^+$ ) in the MOF created an electrostatic attraction with the anionic  $\text{ReO}_4^-$ . As a result, this MOF exhibited a remarkable adsorption capacity for  $\text{ReO}_4^-$ , recorded at  $692 \text{ mg g}^{-1}$ , as per the Langmuir isotherm model.<sup>57</sup>

Wang et al. developed SCU-100, an innovative MOF distinguished by its superior ion selectivity. This MOF is a microporous, cationic structure defined by an 8-fold interpenetrated framework made up of  $[\text{Ag}_2(\text{tipm})_2\text{NO}_3 \cdot 1.5\text{H}_2\text{O}]$  units. In this composition, “tipm” denotes tetrakis[4-(1-imidazolyl)phenyl]methane. SCU-100 comprises a tetradentate neutral N ligand and bicoordinated  $\text{Ag}^+$  sites, with  $\text{NO}_3^-$  serving as a loosely bound counter anion. Exhibiting remarkable hydrolytic stability, SCU-100 retains its crystalline structure in aqueous environments across a broad pH spectrum from 1 to 13 and is resilient against high doses of  $\beta$  and  $\gamma$  radiation. The MOF undergoes a significant structural shift upon interacting with  $\text{ReO}_4^-$ , transitioning from an 8-fold interpenetrated framework with disorganized  $\text{NO}_3^-$  to a 4-fold interpenetrated framework with orderly arranged  $\text{ReO}_4^-$ . This change is driven by the strong binding of each  $\text{ReO}_4^-$  ion by dual  $\text{Ag}^+$  cations and several hydrogen atoms, forming an extensive network of hydrogen bonds. SCU-100 demonstrates a notable affinity for  $\text{ReO}_4^-$ , effectively extracting  $\text{TcO}_4^-$  from water in just 30 min. The MOF boasts an exchange capacity for surrogate  $\text{ReO}_4^-$  as high as  $541 \text{ mg g}^{-1}$ , with a distribution coefficient ( $K_d$ ) surpassing those of previously explored inorganic anion sorbents. Additionally, SCU-100 is highly selective, efficiently capturing  $\text{TcO}_4^-$  even in the presence of a 300-fold excess of competing anions such as  $\text{NO}_3^-$ ,  $\text{SO}_4^{2-}$ ,  $\text{CO}_3^{2-}$ , and  $\text{PO}_4^{3-}$ . Moreover, in practical scenarios, SCU-100 successfully removed up to 87% of  $\text{TcO}_4^-$  from a simulant stream of a Hanford low-activity waste (LAW) melter off-gas scrubber within a mere 2 h, using a solid/liquid ratio of  $5 \text{ mg mL}^{-1}$ . These remarkable characteristics establish SCU-100 as an exceptionally effective and selective material for  $\text{TcO}_4^-$  removal in complex environmental contexts (Figure 3a–d).<sup>58</sup>

The research group furthered their study on MOF materials, specifically focusing on SCU-101, a cationic MOF characterized by its single-crystal nature and the formula  $[\text{Ni}_2(\text{tipm})_2(\text{C}_2\text{O}_4)] \cdot (\text{NO}_3)_2 \cdot 2\text{H}_2\text{O}$ . This material displayed an exceptional ability to selectively remove  $\text{TcO}_4^-$  ions, efficiently functioning even amidst high concentrations of  $\text{NO}_3^-$  and  $\text{SO}_4^{2-}$ . Remarkably, SCU-101 maintained its adsorption capability for  $\text{TcO}_4^-$  ions despite the presence of  $\text{SO}_4^{2-}$  ions in concentrations up to 6000 times higher than  $\text{TcO}_4^-$ . Under these conditions, it achieved an 80% removal efficiency for  $\text{ReO}_4^-$ . The research delved into the sorption mechanism by examining the single-crystal structure of SCU-101 with embedded  $\text{TcO}_4^-$  ions, marking a pioneering instance of a single-crystal structure capturing  $\text{TcO}_4^-$  within a sorbent. Furthermore, density functional theory (DFT) geometry optimizations corroborated these findings, revealing that  $\text{TcO}_4^-$  binds at a site formed by two tipm ligands, aligning with the experimental crystal structure. The sorption isotherm of SCU-101 for  $\text{ReO}_4^-$  closely mirrored the Langmuir model, indicating a maximum uptake capacity of  $217 \text{ mg}$  of  $\text{ReO}_4^-$  per gram, thus underscoring its effectiveness as a sorbent (Figure 3e,f).<sup>59</sup>

Building upon the SCU-101 framework, the team introduced hydrophilic oxalate anions at its nodes, leading to the development of another MOF, SCU-102, characterized by the chemical formula  $\text{Ni}_2(\text{tipm})_3(\text{NO}_3)_4$ . SCU-102 stands out due to the coordination of  $\text{Ni}^{2+}$  ions with six N atoms from distinct tipm ligands. This MOF demonstrated exceptional performance in terms of rapid sorption kinetics, boasting a high capacity of  $291 \text{ mg g}^{-1}$ , and a significant  $K_d$ . Its most remarkable attribute lies in its unparalleled selectivity for the uptake of  $\text{TcO}_4^-$ . The distinctive selectivity of SCU-102 is attributed to the hydrophobic pockets within its structure, leading to an inversion of the typical Hofmeister bias in selectivity. Notably, the sorption properties of SCU-102 toward  $\text{ReO}_4^-$  remained robust even in the presence of substantial amounts of competing anions such as  $\text{NO}_3^-$  and  $\text{SO}_4^{2-}$ . Remarkably, SCU-102 achieved an impressive

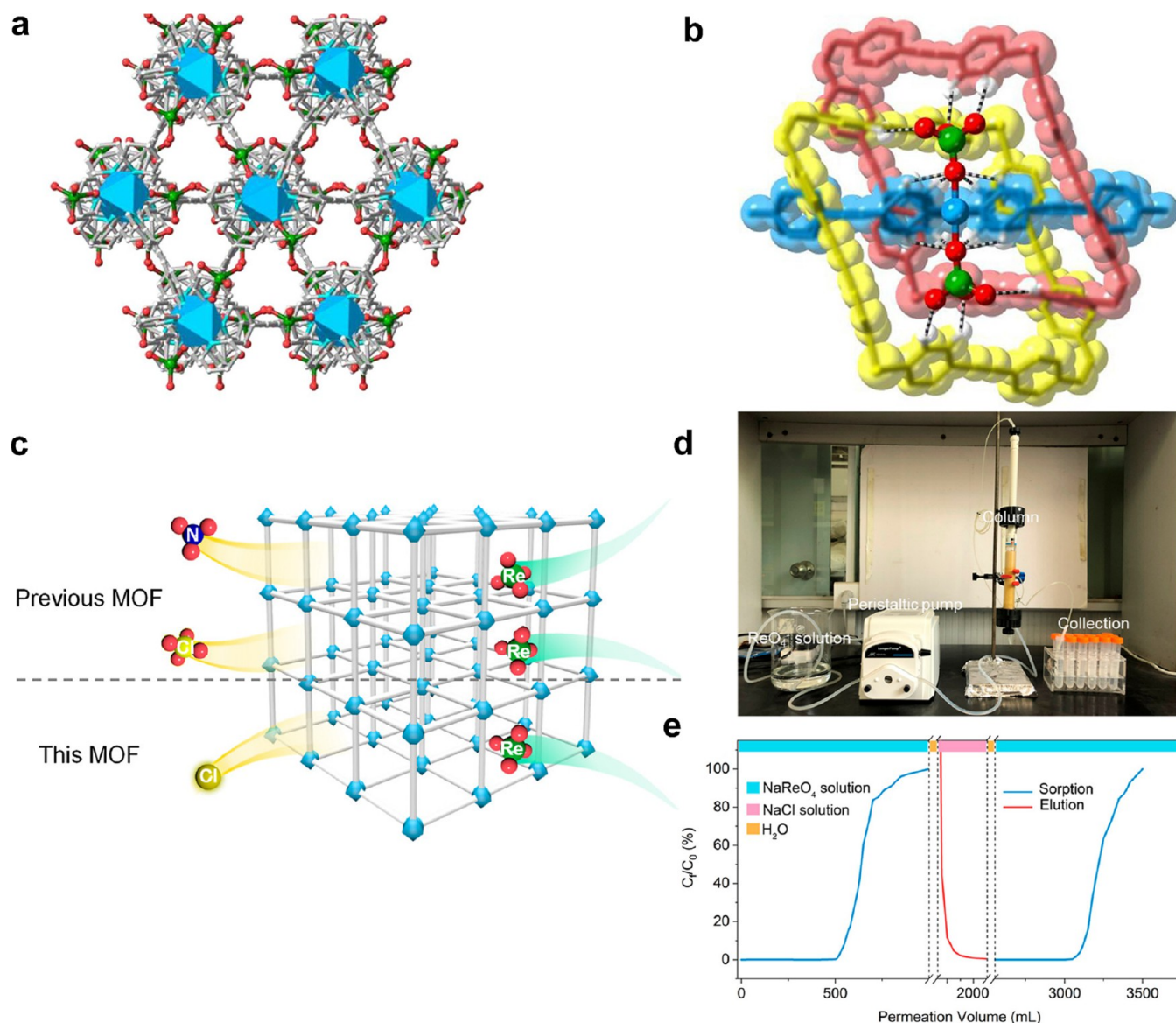


**Figure 4.** (a) 3D framework of ZJU-X6-Tc viewed along the *c* axis. (b) Schematic of <sup>99</sup>TcO<sub>4</sub><sup>-</sup> trapped in the 3-fold interlocking structure of ZJU-X6 through H-bonds. Light gray, cyan, red, white, deep blue, and green colors denote C, N, O, H, Ni, and Tc atoms, respectively. Panels a and b are reproduced from ref 65. Copyright 2021, Elsevier. (c) Schematic representation of released anions by cationic metal–organic framework during elimination of ReO<sub>4</sub><sup>-</sup>. (d) Photograph of the experimental facility for dynamic sorption toward ReO<sub>4</sub><sup>-</sup>. (e) Dynamic sorption and elution curves of ZJU-X4. Panels c–e are reproduced from ref 66. Copyright 2022, American Chemical Science.

removal efficiency of ReO<sub>4</sub><sup>-</sup>, reaching as high as 98.7%, even when NO<sub>3</sub><sup>-</sup> was present at a molar ratio 20 times that of ReO<sub>4</sub><sup>-</sup>. The efficiency remained high at 93.8% even at a NO<sub>3</sub><sup>-</sup>/ReO<sub>4</sub><sup>-</sup> ratio of 100. Furthermore, with SO<sub>4</sub><sup>2-</sup> at a 6000-fold excess, SCU-102 still removed nearly all (99.2%) of the ReO<sub>4</sub><sup>-</sup> ions. These decontamination experiments firmly establish SCU-102 as an optimal Tc adsorbent, showcasing the highest clean-up efficiency reported up to the publication of this paper.<sup>60</sup>

Farha's team achieved significant progress with NU-1000, a Zr<sub>6</sub>-based MOF known for its exceptional adsorption capabilities for ReO<sub>4</sub><sup>-</sup>, attaining a sorption capacity of 210 mg g<sup>-1</sup>. Employing single-crystal X-ray diffraction, they unveiled the distinctive chelating mode of NU-1000, effectively capturing ReO<sub>4</sub><sup>-</sup> in both its small pores and mesopores, alongside two distinct nonchelating modes in each pore type. The large pores within NU-1000 play a pivotal role in facilitating rapid diffusion, providing easy access to the Zr<sub>6</sub> nodes and their substitutionally

labile Zr–OH sites. This unique structural feature empowers NU-1000 to achieve its maximum capacity within a remarkably short span of 5 min, across various concentrations of ReO<sub>4</sub><sup>-</sup>. Importantly, NU-1000 can be easily regenerated after ReO<sub>4</sub><sup>-</sup> adsorption through a simple dilute HCl wash, maintaining an adsorbing capacity of 1.8 ReO<sub>4</sub><sup>-</sup> ions per node over five cycles. Remarkably, the presence of competing anions like Cl<sup>-</sup>, Br<sup>-</sup>, I<sup>-</sup>, and NO<sub>3</sub><sup>-</sup> barely affects ReO<sub>4</sub><sup>-</sup> adsorption, with only SO<sub>4</sub><sup>2-</sup> slightly reducing its effectiveness.<sup>61</sup> In a separate study, Chernikov and his team focused on removing ReO<sub>4</sub><sup>-</sup> from groundwater, particularly in weak acid to near-neutral pH conditions. By anchoring MIL-101-Cr-NO<sub>3</sub> with cetyltrimethylammonium bromide (CTAB), they created a modified adsorbent with rapid kinetics, achieving full capacity of 139 mg g<sup>-1</sup> within 10 min. This efficiency results from a combination of anion-exchange and non-ion-exchange interactions with positively charged moieties of CTAB.<sup>62</sup> Wang and colleagues

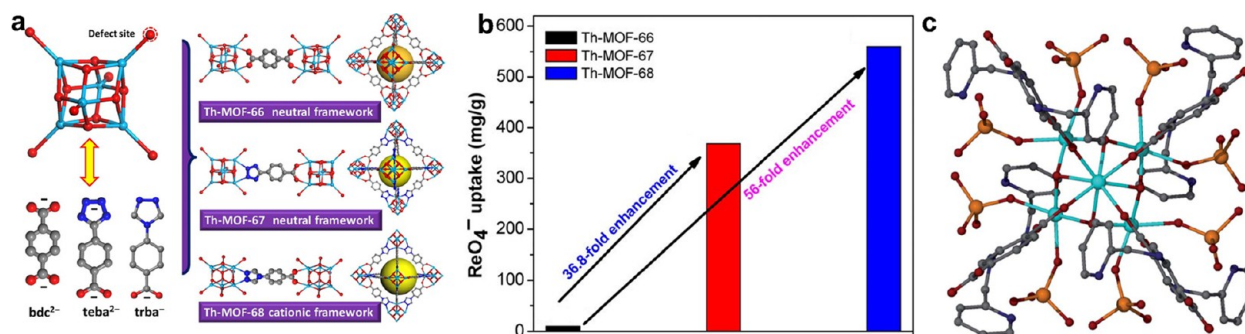


**Figure 5.** (a) View of the structures of Th-MOF-66, Th-MOF-67, and Th-MOF-68. The building units are composed of  $\text{Th}_6\text{O}_4(\text{OH})_4(\text{H}_2\text{O})_6$  cluster and  $\text{bdc}_2^-$ ,  $\text{teba}_2^-$ , or  $\text{trba}^-$  linkers. From the consideration of charge balance, Th-MOF-66 ( $\text{Th}_6\text{O}_4(\text{OH})_4(\text{H}_2\text{O})_6(\text{bdc})_{12}$ ) and Th-MOF-67 ( $\text{Th}_6\text{O}_4(\text{OH})_4(\text{H}_2\text{O})_6(\text{teba})_{12}$ ) are neutral frameworks, while Th-MOF-68 ( $[\text{Th}_6\text{O}_4(\text{OH})_4(\text{H}_2\text{O})_6(\text{trba})_{12}][\text{Cl}]_6$ ) is a cationic framework with the counterpart of  $\text{Cl}^-$  ions. (b) Comparison of  $\text{ReO}_4^-$  adsorption capacity for Th-MOF-66, Th-MOF-67, and Th-MOF-68. Panels a and b are reproduced from ref 67. Copyright 2021, Tsinghua University Press and Springer-Verlag. (c) Representation of the  $\text{Zr}_6$  unit in MOR-2/ $\text{ReO}_4^-$  highlighting the presence of eight monodentate  $\text{ReO}_4^-$  ligands. Color code: Zr, sky blue; O, red; C, gray; N, blue; Re, orange; Cl, green. Reproduced from ref 68. Copyright 2018, Royal Society of Chemistry.

developed BUC-17, a water-stable MOF utilizing 1,3,5-tris(1-imidazolyl)benzene and cobalt sulfate ( $\text{CoSO}_4$ ). BUC-17, featuring replaceable  $\text{SO}_4^{2-}$  ions, exhibited a remarkable sorption capacity of  $401.9 \text{ mg g}^{-1}$  for  $\text{ReO}_4^-$ . It demonstrated exceptional selectivity toward  $\text{ReO}_4^-$ , maintaining over 97% removal efficiency even with a molar ratio of  $\text{NO}_3^-/\text{ReO}_4^-$  of 100:1, and over 96% efficiency at a  $\text{SO}_4^{2-}/\text{ReO}_4^-$  ratio of 6000:1, validating its efficiency in  $\text{ReO}_4^-$  removal from waste streams.<sup>63</sup>

Xiao's team synthesized a series of cationic, pyrimidyl-based MOFs, notable for their positively charged framework and hydrophobic 1D channels. Among these, ZJU-X11, made from 1,4-di(pyrimidin-5-yl)benzene and  $\text{AgNO}_3$ , demonstrated a remarkable maximum sorption capacity for  $\text{ReO}_4^-$ , reaching  $518 \text{ mg g}^{-1}$ . This MOF impressively maintained over 80% removal efficiency for  $\text{ReO}_4^-$  with high concentrations of competing ions, such as 500 molar equivalents of  $\text{SO}_4^{2-}$  and 100 molar equivalents of  $\text{NO}_3^-$ .<sup>64</sup> In another innovative endeavor, Xiao and collaborators developed ZJU-X6, a cationic MOF with a unique 3-fold interlocking structure, using tetrakis(4-(4-pyridyl)ethynyl)phenyl)ethene and  $\text{Ni}^{2+}$  nodes. The accessible  $\text{Ni}^{2+}$  nodes on the ZJU-X6 efficiently capture  $^{99}\text{TcO}_4^-$  through Ni-OTc coordination, as evidenced by Pair Distribution Function (PDF) analysis and the single-crystal structure of ZJU-X6-Tc. Its 3-fold interlocking structure, combined with a 6-coordination mode and replaceable  $\text{H}_2\text{O}$  molecules, amplifies the positive charge density of the framework. This augmentation contributes to exceptional sorption properties specifically tailored for  $^{99}\text{TcO}_4^-$ , surpassing the capacity of other nickel-node. Notably, the adsorption of ZJU-X6 for  $\text{ReO}_4^-$  is fully reversible, with the adsorbed ions effectively removable using  $\text{NaNO}_3$  elution (Figure 4a,b).<sup>65</sup> Despite these advancements in  $\text{TcO}_4^-$  removal using sorbents, the issue of potential secondary contamination from exchanged counterions (like  $\text{NO}_3^-$ ) in cationic MOFs was underexplored. Addressing this, Xiao's team synthesized ZJU-X4, another cationic MOF, but with a key distinction: it incorporates  $\text{Cl}^-$  as counterions, potentially reducing the risk of secondary contamination. The fabrication of ZJU-X4 involved tris(4-pyridylethynyl)triphenylamine and  $\text{NiCl}_2$ . Ion chromatography demonstrated a one-to-one correspondence between the amount of  $\text{Cl}^-$  released and the target ions absorbed, elucidating the ion-exchange dynamics in ZJU-X4. Detailed pair distribution function analysis further

illuminated the structural changes in ZJU-X4 upon  $\text{ReO}_4^-$  absorption, vividly showcasing the underlying anion-exchange mechanism. ZJU-X4 displayed an uptake capacity of  $395 \text{ mg g}^{-1}$  for  $\text{ReO}_4^-$ , with dynamic sorption experiments indicating that  $\text{ReO}_4^-$  could be effectively and reversibly removed and recovered using a 3M NaCl solution. This highlights the potential of ZJU-X4 for practical applications, especially where efficient and reversible sorption is crucial (Figure 4c–e).<sup>66</sup> Luo and team focused on the impact of ligands on the radionuclide removal capabilities of thorium-based organic frameworks, particularly for  $\text{TcO}_4^-$ . By employing coordination modulation, they transitioned from carboxylate (terephthalate acid) to tetrazolate (4-(tetrazol-5-yl)benzoate) and then to triazolate (4-(1,2,4-triazol-4-yl)benzoate) linkers, leading to the creation of Th-MOF-66, Th-MOF-67, and Th-MOF-68, respectively. Th-MOF-66 showed low  $\text{ReO}_4^-$  uptake, whereas isorecticular MOFs Th-MOF-67 and Th-MOF-68 exhibited a substantial increase, with 36.8-fold and 56-fold enhancements, respectively. In-depth analysis, including single-crystal structure and theoretical calculations, indicated that the increased uptake in Th-MOF-67 was due to coordination interactions, and in Th-MOF-68, it was a result of both coordination interactions and anion exchange (Figure 5a,b).<sup>67</sup>

While the aforementioned certain MOF materials exhibit stability in neutral environments, the extraction of  $^{99}\text{TcO}_4^-$  from highly acidic solutions, such as those found in used nuclear fuel, is crucial not only for the efficient removal of  $^{99}\text{TcO}_4^-$  during PUREX process but also for significantly reducing the environmental impact of  $^{99}\text{Tc}$  discharge. Manos and team developed two zirconium-based MOFs, MOR-1 and MOR-2, utilizing 2-aminoterephthalic acid and 2-((pyridin-1-ium-2-yl)methyl)ammonio)terephthalate as organic ligands, respectively. Particularly, MOR-2 demonstrated exceptional sorption capacities for  $\text{ReO}_4^-$  and  $\text{TcO}_4^-$  anions (up to  $4.1 \pm 0.4 \text{ mmol g}^{-1}$ ), setting a new standard for MOF-based sorbents at the time. This high capacity is attributed to the effective interaction between the anionic species and the ammonium/pyridinium sites in the MOF, and the incorporation of these anions into the  $\text{Zr}_6$  core of MOR-2. Remarkably, MOR-2 maintained its exceptional sorption efficiency even in highly acidic environments (1 M  $\text{HNO}_3$ ), highlighting its potential for the remediation of acidic nuclear waste. Moreover, a composite form of MOR-2, combined with alginate acid (HA), was utilized

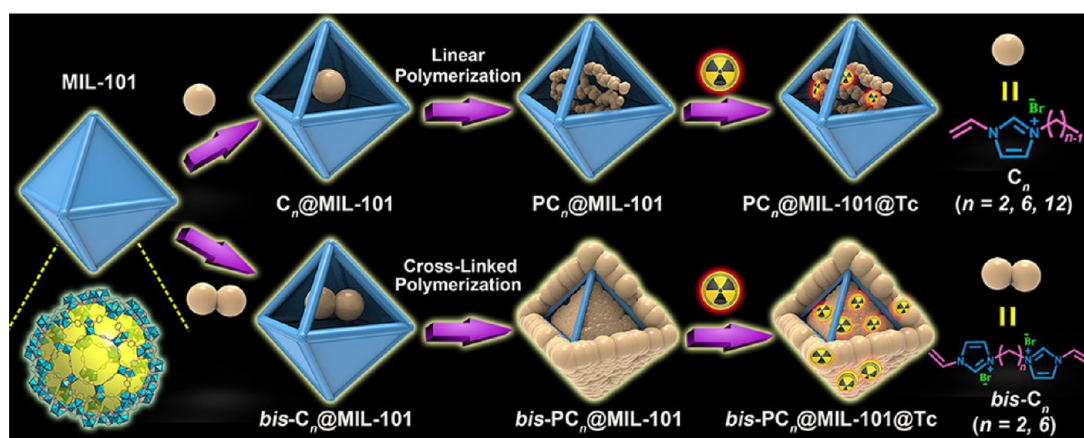


**Figure 6.** Designing strategy of polyILs@MOFs composites for radionuclide sequestration, by in-situ polymerization of the encapsulated imidazolium-based ILs in the pores of MOFs. (MIL-101 was chosen as the representative MOF here.) Reproduced from ref 70. Copyright 2020, American Chemical Society.

as an ion-exchange column, showcasing its ability to completely remove  $\text{ReO}_4^-$  from water. This composite demonstrated efficient regenerability and reusability, retaining its initial sorption capacity through multiple cycles (Figure 5c).<sup>68</sup> In a separate advancement, a cationic MOF named SCNU-Z1-Cl was synthesized by reacting bifunctional tripodal ligands (HDITP = 3,5-di(1*H*-imidazol-1-yl)phenyl)-2*H*-tetrazole) with  $\text{Ni}^{2+}$  ions. Featuring tubular channels, this MOF exhibited outstanding adsorption performance for various oxo-anion pollutants, including  $\text{MnO}_4^-$ ,  $\text{Cr}_2\text{O}_7^{2-}$ ,  $\text{CrO}_4^{2-}$ , and  $\text{ReO}_4^-$ .<sup>69</sup>

Du and collaborators innovatively introduced ion-exchangeable sites into MOFs through a cutting-edge host–guest assembly method. This approach entails the in-situ polymerization of ionic monomers within the pore channels of a MOF host. Specifically, they encapsulated a series of vinyl-functionalized imidazolium-based ionic liquids into the pores of MIL-101, followed by in-situ polymerization. The resulting optimized composite exhibited rapid sorption kinetics (less than 30 s), remarkable durability over multiple regeneration cycles (exceeding 30 cycles), and outstanding adsorption performance for  $\text{TcO}_4^-$ , even under highly acidic conditions and in simulated recycle streams. An illustrative example of its effectiveness is observed in the removal of 74% of  $\text{ReO}_4^-$  from a simulated Hanford LAW melter recycle stream. This advancement not only expands the application scope of MOFs for radionuclide sequestration but also provides a versatile blueprint for designing high-performance composites for sorption applications (Figure 6).<sup>70</sup>

Li and collaborators have successfully developed two highly durable cationic Zr-MOFs, namely, Zr-tcbp-Me and Zr-tcpp-Me, showcasing remarkable stability in challenging aqueous environments. Here, tcbp and tcpp denote 4,4',6,6'-tetracarboxy-2,2'-bipyridine and 2,3,5,6-tetrakis(4-carboxyphenyl)pyrazine, respectively. These MOFs were synthesized through solvothermal reactions, followed by postsynthetic N-methylation of the tetracarboxylic ligands. Remarkably, these MOFs demonstrated exceptional stability, enduring 3 days in 6 M HCl and 24 h in pH 13 NaOH solutions, as confirmed by their powder X-ray diffraction (PXRD) patterns. Their uptake capacities for  $\text{ReO}_4^-$  are noteworthy, with Zr-tcbp-Me and Zr-tcpp-Me achieving 128 and 121  $\text{mg g}^{-1}$ , respectively, approximating 76% and 99% of their theoretical capacities. This efficiency is attributed to the preferential binding of the

relatively soft anion  $\text{ReO}_4^-$  to the soft  $\text{N}^+-\text{CH}_3$  cationic centers in the MOFs, an interpretation supported by the Pearson hard/soft acid/base theory.<sup>71</sup>

Cationic pyridine and imidazolium rings often face challenges with alkaline stability, becoming susceptible to nucleophilic attacks by  $\text{OH}^-$  ions in alkaline environments, which can lead to ring-opening reactions. This issue is particularly significant in contexts like the treatment of legacy defense waste at the SRS. Addressing this, Wang and his team developed SCU-103, a 2D cationic MOF that demonstrates remarkable resilience in alkaline conditions. SCU-103 is constructed using a tridentate N ligand, tris[4-(1*H*-imidazol-1-yl)phenyl]amine (tipa), and  $\text{Ni}^{2+}$  ions. It showcases superior radiation resistance and hydrolytic stability, attributed to the steric crowding at the metal centers and the encapsulation within concave–convex layers by the nonplanar tipa ligands. The extensive conjugated structure of tipa also helps stabilize radiation-induced radicals, enhancing its resistance to  $\text{H}_2\text{O}$ ,  $\text{OH}^-$ , and radiation. Its stability was confirmed through unaltered PXRD patterns after being subjected to pH levels from 3 to 14 and  $\beta$  and  $\gamma$  radiation of 100 and 200 kGy, respectively. SCU-103 is not only stable but also efficient in contaminant removal. It can eliminate approximately 92% of  $^{99}\text{TcO}_4^-$  within 30 s, and over 95% within 5 min, at a molar ratio of about 6:1 (SCU-103 to  $^{99}\text{TcO}_4^-$ ). This removal process is driven by chemical adsorption and fits a pseudo-second-order kinetic model. SCU-103 also possesses a high uptake capacity, with a maximum anion-exchange capacity of  $318 \pm 8 \text{ mg g}^{-1}$ , as determined by fitting its sorption isotherm to the Langmuir model. SCU-103 displays remarkable selectivity and affinity for  $\text{ReO}_4^-/^{99}\text{TcO}_4^-$  ions, even in environments with a high concentration of competing anions like  $\text{NO}_3^-$  or  $\text{SO}_4^{2-}$ . Its removal efficiency remains above 97% for  $\text{NO}_3^-$  to  $\text{ReO}_4^-$  molar ratios ranging from 1:1 to 20:1. Impressively, SCU-103 still captures over 88% of  $\text{ReO}_4^-$  ions even at a 100:1 molar ratio. In settings with a 6000-fold excess of  $\text{SO}_4^{2-}$ , SCU-103 maintains high  $\text{ReO}_4^-$  removal efficacy (82%). Furthermore, SCU-103 exhibits an impressive removal efficiency of over 99% for  $\text{ReO}_4^-$  (200 ppm) in solid–liquid ratios of  $10 \text{ mg mL}^{-1}$  and above, at a pH level of 14. These promising findings prompted testing SCU-103 for the removal of  $^{99}\text{TcO}_4^-$  from real SRS tank waste with 1.88 M  $\text{OH}^-$ , 1.82 M  $\text{NO}_3^-$ , 0.489 M  $\text{NO}_2^-$ , 0.04 M  $\text{SO}_4^{2-}$ , and 0.24 M  $\text{CO}_3^{2-}$ , alongside various radionuclides like  $^{137}\text{Cs}$ ,  $^{90}\text{Sr}$ ,  $^{238}\text{Pu}$ , and  $^{99}\text{Tc}$ . With a phase ratio of  $40 \text{ mg mL}^{-1}$ , SCU-103

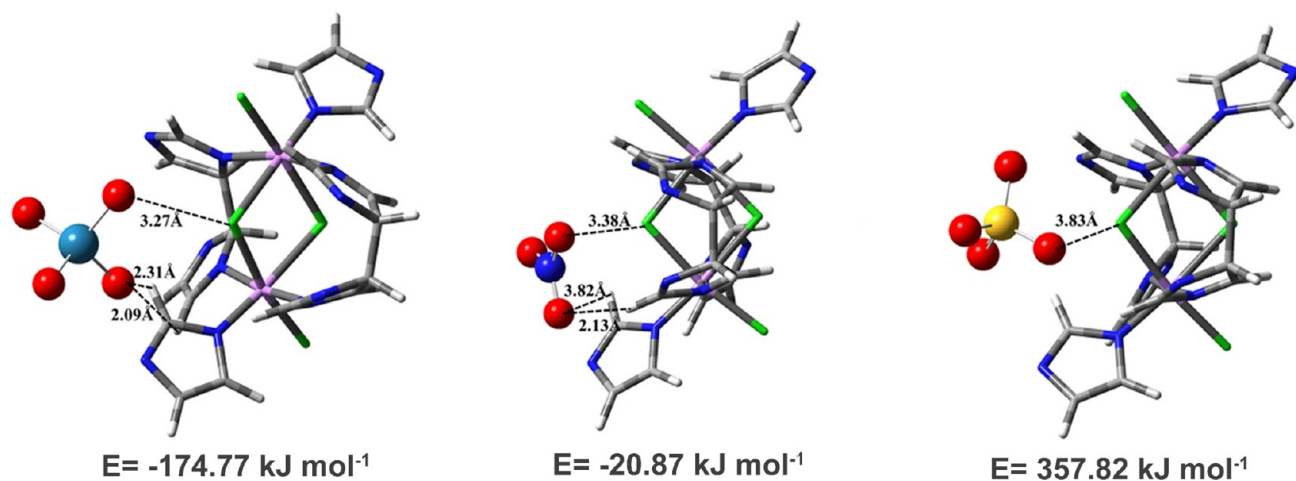


**Figure 7.** Optimized structures of the Mn-MOF fragment binding with different anions and the corresponding binding energies. Reproduced from ref 74. Copyright 2022, The Authors.

successfully removed 90% of the  $^{99}\text{TcO}_4^-$  from the solution within 3 h. This achievement is groundbreaking, marking the first successful testing of a MOF material under genuinely challenging conditions encompassing high alkalinity, ionic strength, and strong radiation. These results highlight SCU-103 as an alkaline-stable cationic MOF excelling in capturing  $^{99}\text{TcO}_4^-$  in real SRS high-level waste (HLW) scenarios, potentially addressing long-standing issues in legacy waste partitioning. This study introduces a new paradigm for designing adsorbents, opening avenues for future nuclear waste remediation.<sup>72</sup>

Xiao and colleagues engineered a cationic MOF, Ag-TPPE, notable for its exceptional alkaline resistance. This MOF is synthesized by assembling 1,1,2-tetrakis(4-pyridylphenyl)ethylene (TPPE) with  $\text{Ag}^+$  ions. A significant feature of Ag-TPPE is its rapid, room-temperature synthesis, achievable through stirring or sonication. Its step-by-step process enables immediate crystal formation, even under direct mixing conditions. Ag-TPPE demonstrates remarkable stability, retaining its crystallinity and structural integrity even under the harsh conditions of strong bases (8 M) and considerable radiation exposure. The  $\text{ReO}_4^-$  uptake capacity of Ag-TPPE is high, reaching  $251 \text{ mg g}^{-1}$  as per the Langmuir model. In dynamic sorption experiments, a column containing 100 mg of Ag-TPPE and excess quartz effectively removed over 99.97% of  $\text{ReO}_4^-$  from a 400 mL solution with 30 ppm  $\text{ReO}_4^-$ , lowering the concentration to under 10 ppb. DFT calculations suggest that  $\text{TcO}_4^-$  is stabilized in a large cavity of Ag-TPPE through dense hydrogen bonds, demonstrating the selectivity of the MOF. Ag-TPPE maintains over 64%  $\text{ReO}_4^-$  removal efficiency even with a 5000-fold excess of  $\text{NO}_3^-$ . Additionally, it showed significant efficiency in removing  $\text{ReO}_4^-$  from a simulated SRS waste solution, with a 37% removal rate at a 1:1 solid/liquid ratio, which can be increased to up to 90% at a 10:1 ratio. This efficiency represents a new standard in sorbent performance for extracting  $\text{TcO}_4^-$  in highly alkaline and high ionic strength conditions.<sup>73</sup>

In a different study, Qiu et al. developed a MOF material named Mn-MOF, tailored for stability in highly alkaline nuclear fuel solutions. Their approach involved incorporating halogens into a 2D MOF composed of tipa and manganese chloride ( $\text{MnCl}_2$ ). This MOF is characterized by abundant Mn–Cl bonds and orderly hydrophobic pore channels, conferring high

resistance to  $\text{OH}^-$  attack and a tendency to adsorb hydrophobic  $\text{ReO}_4^-$  ions. Mn-MOF demonstrates exceptional selectivity for  $\text{ReO}_4^-$ , even with high concentrations of  $\text{NO}_3^-$  and  $\text{SO}_4^{2-}$ . For instance, Mn-MOF achieved up to 68% removal of  $\text{ReO}_4^-$ , even when the molar ratio of  $\text{NO}_3^-/\text{ReO}_4^-$  reaches 500. Furthermore, it maintained a 64.0% removal efficiency when the concentration of  $\text{SO}_4^{2-}$  was 1000 times that of  $\text{ReO}_4^-$ . Notably, Mn-MOF also showed remarkable effectiveness in removing  $\text{ReO}_4^-$  from strongly basic solutions (1.3 M NaOH), achieving a removal efficiency of 67% with a phase ratio of 10 (Figure 7).<sup>74</sup>

Subsequently, the same research group developed two isostructural MOFs, NCU-3-Cl and NCU-3-Br, demonstrating resistance to alkaline conditions. These MOFs are synthesized by combining  $\text{ZnX}_2$  with tipa. Their findings indicated that the type of halogen atom in the MOF structure significantly influences its adsorption capabilities for  $\text{ReO}_4^-/\text{TcO}_4^-$ . NCU-3-Br, in particular, stands out for its superior adsorption performance, attributed to the lower electronegativity of Br atoms, which enhances the formation of  $\sigma$ -holes. As a result, NCU-3-Br shows an adsorption capacity of  $483 \text{ mg g}^{-1}$ , which is more than double that of NCU-3-Cl. In 1 M NaOH solutions, NCU-3-Br is remarkably efficient at removing  $\text{ReO}_4^-$ . At a phase ratio of  $5 \text{ mg mL}^{-1}$ , it removes about 92.1% of  $\text{ReO}_4^-$ , and this efficiency significantly increases to 98.8% when the phase ratio is raised to  $10 \text{ mg mL}^{-1}$ . These results underline the potential of NCU-3-Br as an effective sorbent for  $\text{ReO}_4^-$  in alkaline conditions.<sup>75</sup>

Monitoring  $\text{ReO}_4^-/\text{TcO}_4^-$  concentrations in environmental water samples is essential for effective adsorption and removal strategies. To address this, Qiu and collaborators have developed NCU-2, a cationic fluorescent MOF, using a novel interpenetration method. This framework is constructed from a flexible tridentate N-containing ligand, tris[4-(1H-imidazole-1-yl)phenyl]amine, combined with  $\text{Ag}^+$  ions. NCU-2 is notable for its complex 14-fold interpenetrated structure, which ensures excellent chemical stability even in acidic environments like 0.5 M  $\text{HNO}_3$ . A significant feature of NCU-2 is its abundance of unsaturated Ag metal sites, strategically located along the 1D pore channels. These sites enhance positive charge density of the framework and facilitate the rapid movement of guest molecules, increasing their interactions within the framework. This attribute makes NCU-2 particularly effective in targeting



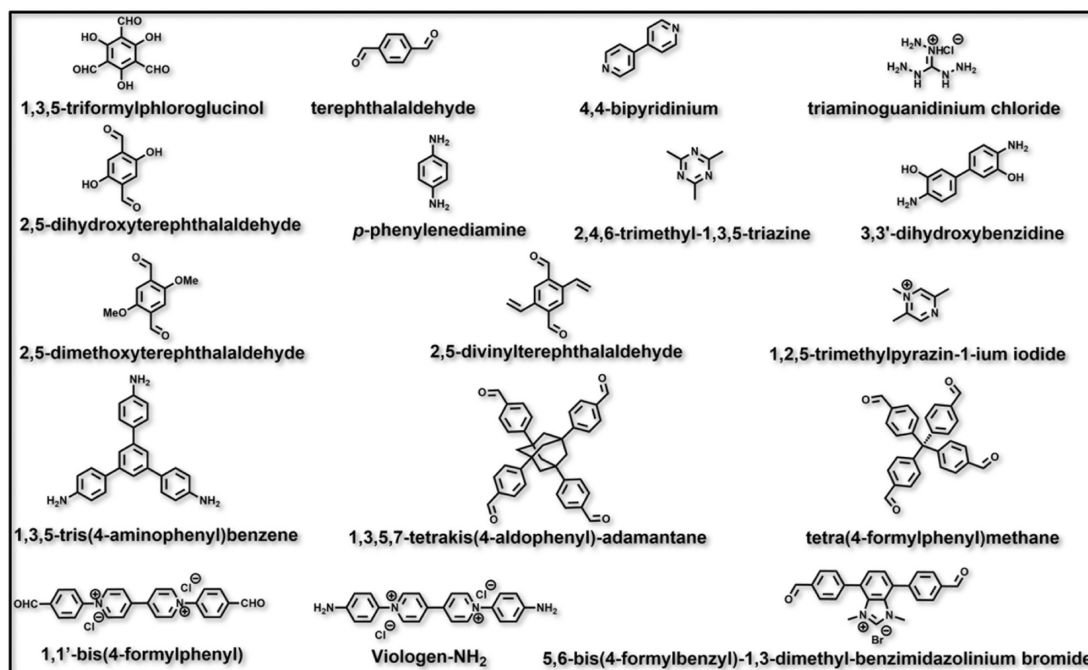


**Figure 8.** Molecular structures of the monomers used in constructing the COFs discussed in this Review.

$\text{ReO}_4^-$ . Upon encountering  $\text{ReO}_4^-$ , NCU-2 forms a non-fluorescent complex, leading to a substantial quenching of its fluorescence signal. This response is utilized in the sensitive detection of  $\text{ReO}_4^-$ , as demonstrated in simulated Hanford waste, where NCU-2 showcases a linear detection range of 0.2–200  $\mu\text{M}$  and a remarkably low detection limit of 66.7 nM. Furthermore, NCU-2 displays a high  $\text{ReO}_4^-$  uptake capacity, measured at 541  $\text{mg g}^{-1}$ , along with rapid sorption kinetics. These characteristics make NCU-2 a highly promising material for applications in waste monitoring and emergency remediation, especially for trace-level detection and quantification of  $\text{ReO}_4^-$  in challenging environments.<sup>76</sup>

## ■ COF-BASED SORBENTS

COFs are materials composed of 2D or 3D networks formed through reactions between organic precursors. These reactions result in strong covalent bonds, yielding porous, stable, and crystalline structures. COFs have comparable advantages to MOFs in terms of structure–property design. Despite typically exhibiting more limited long-range order compared to MOFs, the creation of single-crystalline COFs has been achieved in certain cases. The molecular structures of the monomers used in constructing the COFs and the structures of the resulting COFs discussed in this Review are illustrated in Figures 8 and 9. Ghosh and colleagues have ingeniously designed a novel hybrid material for anion exchange. This material incorporates nanosized cationic metal–organic polyhedra (MOPs, denoted as  $\{[\text{Cp}_3\text{Zr}_3\text{O}(\text{OH})_3]_4(\text{NH}_2\text{-BDC})_6\}\cdot\text{Cl}_4$ ) within a COF framework. The COF is constructed using 1,3,5-triformylphloroglucinol (Tp) and *p*-phenylenediamine, which are chosen specifically for their ability to create sorption sites targeting toxic oxoanions. The synthesized hybrid material demonstrates exceptional performance in the rapid and selective removal of various toxic oxoanions, including  $\text{ReO}_4^-$ . It is particularly effective in environments with a high concentration of other interfering anions, showing an ability to reduce the concen-

tration of the toxic oxoanions to levels well below the limits permissible in drinking water (Figure 10).<sup>77</sup>

Shi and their research team have innovated a postsynthetic grafting method that employs ionizing radiation to attach an imidazolium-based ionic liquid, specifically 1-vinyl-3-ethylimidazolium bromide ( $\text{C}_2\text{vimBr}$ ), to a vinyl-rich COF, known as TbDa-COF. The resulting products are labeled as  $[\text{C}_2\text{vimBr}]_{x\%}\text{-TbDa-COF}$ , where  $x\%$  indicates the grafting yield. The team has adeptly utilized  $\gamma$ -ray radiation to precisely control the integration of charged imidazolium groups within the COF structure. The precise control employed significantly amplifies the capacity of the COF for  $\text{ReO}_4^-$  uptake, achieving an impressive 952  $\text{mg g}^{-1}$  with notable features such as high selectivity and rapid absorption kinetics. The exceptional porosity and nanofiber architecture of the sorbent contribute to its high effectiveness, particularly evident in dynamic column experiments. In these tests, the COF efficiently removes over 99.98% of  $\text{ReO}_4^-/\text{TcO}_4^-$  from solutions, reducing their concentration to below 0.8 ppb—far lower than the maximum permissible limit of World Health Organization for heavy metal ions in drinking water. Remarkably, the performance of the COF remains consistent even after four adsorption–desorption cycles, maintaining high efficiency when regenerated with a 1 M KBr solution. These attributes underscore the potential of  $[\text{C}_2\text{vimBr}]_{x\%}\text{-TbDa-COF}$  in practical applications, especially for extracting  $\text{TcO}_4^-$  from environmental and nuclear waste (Figure 11).<sup>78</sup>

Additionally, the team extended their  $\gamma$  radiation modification technique to develop a unique 3D COF with a superhydrophobic phosphonium-containing coating, named 3DCOF-g-VBPPH<sub>3</sub>Cl. This innovative approach significantly boosts the capacity of the COF to attract less hydrophilic and charge-dispersed anionic pollutants like  $\text{TcO}_4^-$ . It addresses the limitations typically associated with cationic frameworks and mitigates the Hofmeister bias. The modified 3D COF demonstrates a strong affinity for the oxoanion  $\text{TcO}_4^-$  due to its carefully regulated surface hydrophobicity, illustrating its

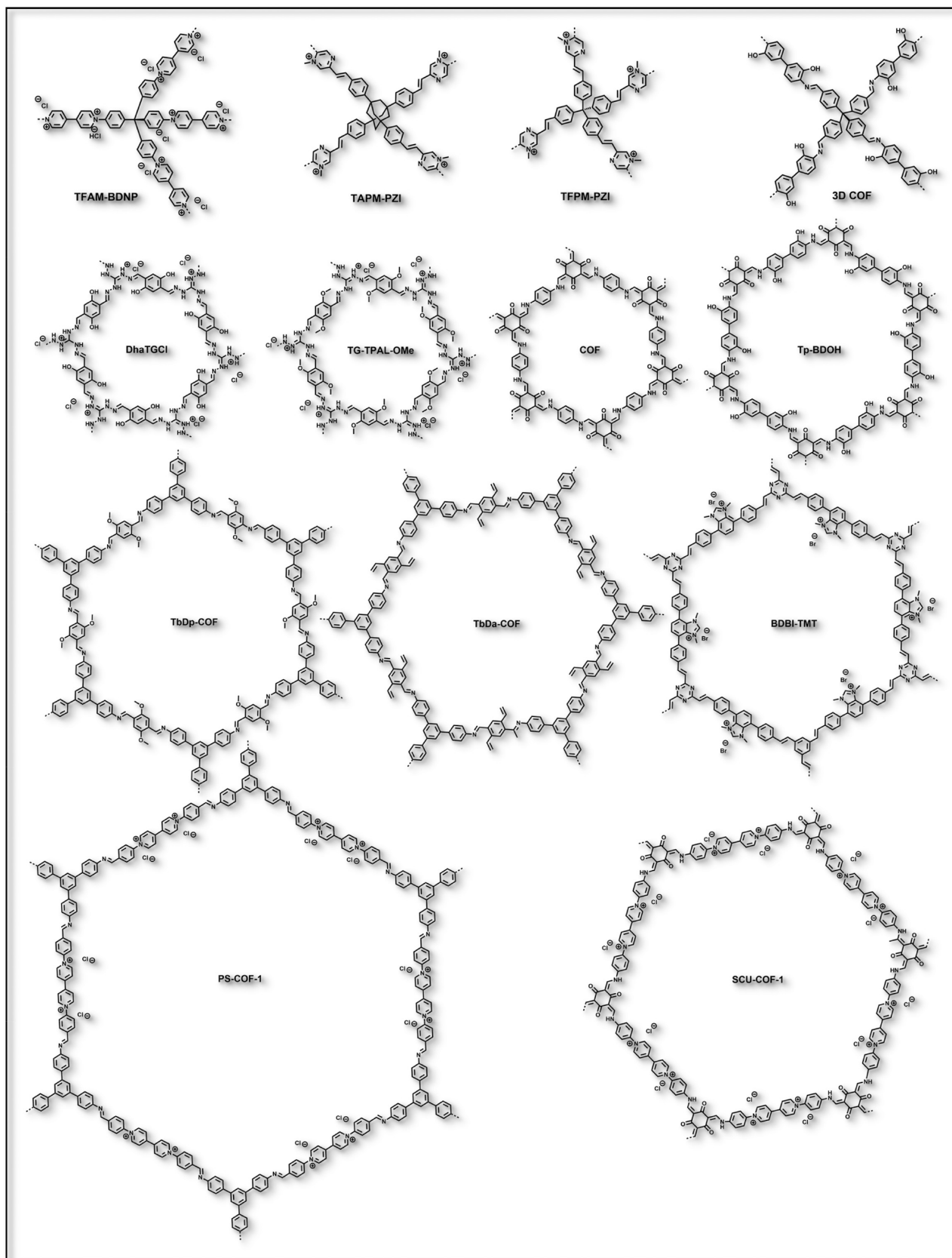


**Figure 9.** Chemical structures of the COFs discussed in this Review.

potential in advanced environmental remediation applications. The 3DCOF-g-VBPPH<sub>3</sub>Cl material has undergone thorough testing in both tap water and simulated groundwater,

showcasing its remarkable ability to sequester contaminants. These tests have demonstrated an exceptional removal efficiency of up to 99.995%, setting a new benchmark with a  $K_d$  of  $1.0 \times 10^8$

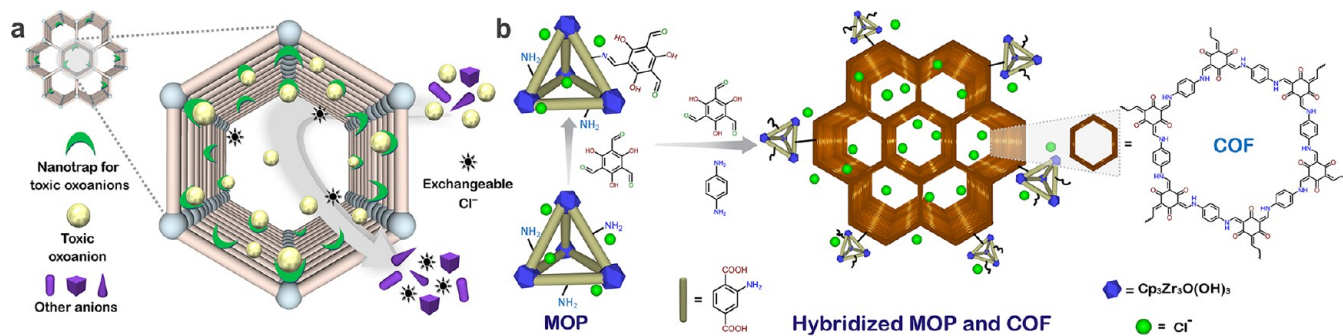


**Figure 10.** (a) Schematic representation of selective capture of toxic oxoanions by a nanotrap grafted anion-exchangeable hybrid material. (b) Schematic illustration of the synthesis of anion-exchangeable hybrid material. Reproduced from ref 77. Copyright 2020, American Chemical Society.

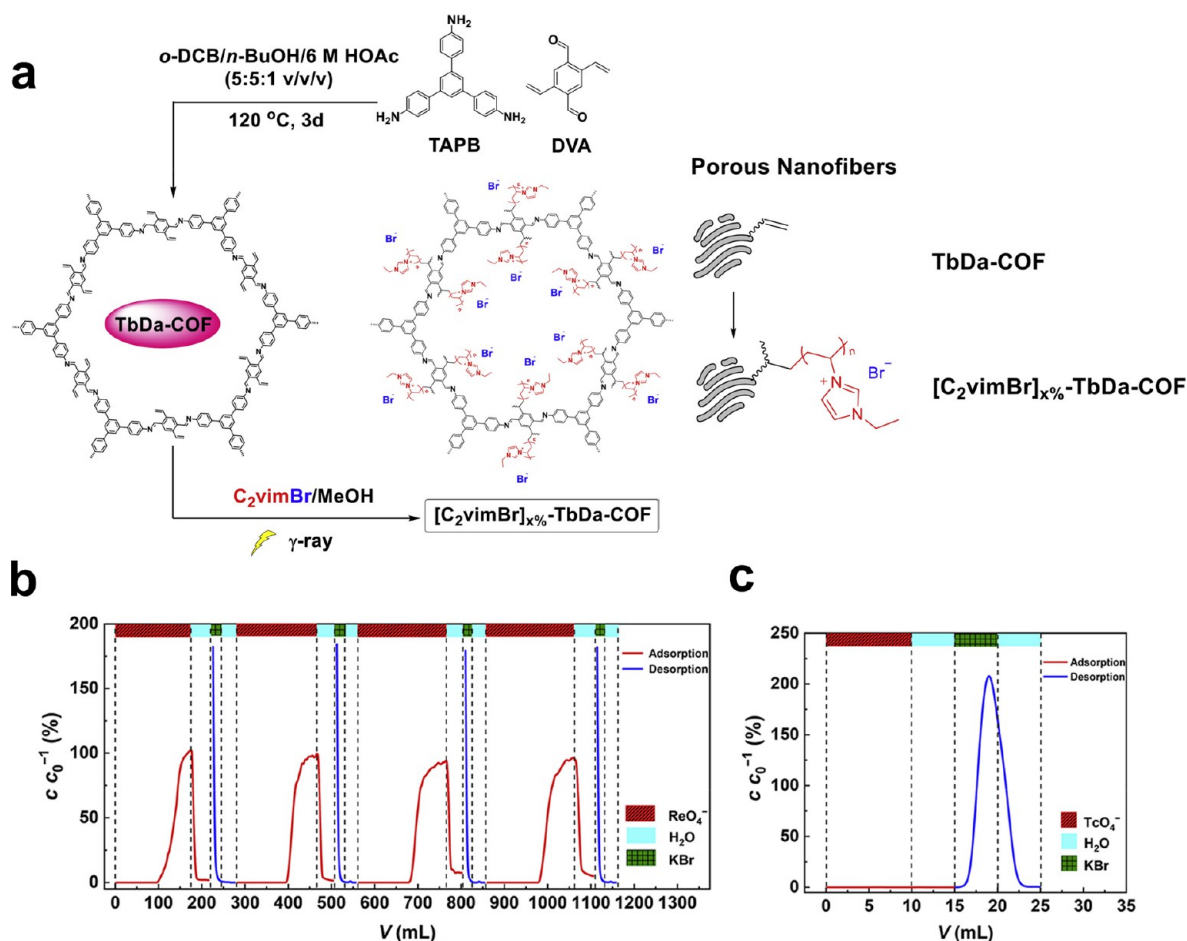


**Figure 11.** (a) Synthetic procedures for TbDa-COF and [C<sub>2</sub>vimBr]<sub>x</sub>%-TbDa-COF. (b) Dynamic elution curve of [C<sub>2</sub>vimBr]<sub>16</sub>%-TbDa-COF packed column for ReO<sub>4</sub><sup>-</sup> separation, with the concentrations of ReO<sub>4</sub><sup>-</sup> measured by ex-situ ICPAES. (c) Dynamic elution curve of [C<sub>2</sub>vimBr]<sub>16</sub>%-TbDa-COF packed column for TcO<sub>4</sub><sup>-</sup> separation. The feed solution was ReO<sub>4</sub><sup>-</sup> or TcO<sub>4</sub><sup>-</sup> aqueous solutions containing 25 ppm Re or 10 ppm Tc, which was pumped through the column at a flow rate of 1.0 mL min<sup>-1</sup>. Reproduced from ref 78. Copyright 2020, Elsevier.

mL g<sup>-1</sup>. This material exhibits a notable selectivity for TcO<sub>4</sub><sup>-</sup>, effectively distinguishing it from other common anions such as Cl<sup>-</sup>, NO<sub>3</sub><sup>-</sup>, and SO<sub>4</sub><sup>2-</sup>. To evaluate its performance against a backdrop of competing anions, the sorption of ReO<sub>4</sub><sup>-</sup> was examined under high concentrations of NO<sub>3</sub><sup>-</sup>, SO<sub>4</sub><sup>2-</sup>, and PO<sub>4</sub><sup>3-</sup>. Impressively, even when faced with challenging concentration ratios with NO<sub>3</sub><sup>-</sup>/ReO<sub>4</sub><sup>-</sup>, SO<sub>4</sub><sup>2-</sup>/ReO<sub>4</sub><sup>-</sup>, and PO<sub>4</sub><sup>3-</sup>/ReO<sub>4</sub><sup>-</sup> at 100:1, 6000:1, and 6000:1, respectively, the material maintained high removal rates of 80.7%, 93.9%, and 92.5%, respectively. This performance is particularly significant considering the high solubility and environmental mobility of

TcO<sub>4</sub><sup>-</sup>, which pose a substantial risk to groundwater, aquatic ecosystems, and human health. The effectiveness of 3DCOF-*g*-VBPPH<sub>3</sub>Cl was further confirmed in simulated Beishan groundwater spiked with ReO<sub>4</sub><sup>-</sup>, where it achieved removal efficiencies between 94.2% and 98.4% for various initial Re concentrations, despite the presence of other anions in much higher concentrations. This evidence underscores the potential of this material for practical application, especially for selectively removing TcO<sub>4</sub><sup>-</sup> from contaminated water sources. The adsorption kinetics of 3DCOF-*g*-VBPPH<sub>3</sub>Cl were also rigorously tested using simulated Beishan groundwater containing 12.5

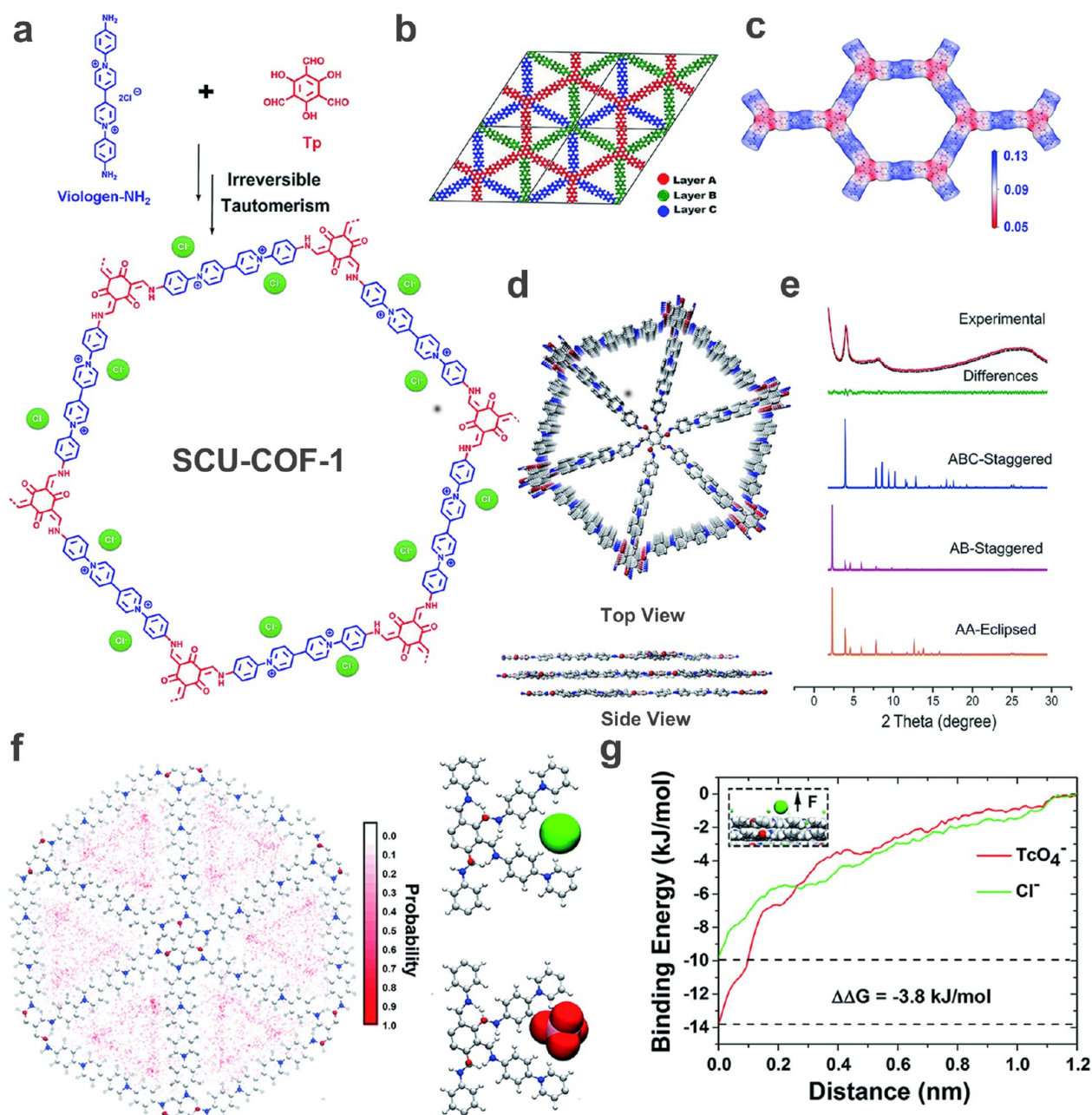


**Figure 12.** (a) Synthesis of SCU-COF-1. (b) Expanded R3 symmetric unit cell matching with the ABC-staggered stacking model (red for layer A, green for layer B, and blue for layer C). (c) Electrostatic potential distribution mapping of SCU-COF-1. (d) Top view and side view of SCU-COF-1 (chloride ions and hydrogen atoms omitted for clarity). (e) Experimental PXRD pattern of SCU-COF-1 (red line), Pawley refined pattern (black dots), difference curve between experimental and refined pattern (green line), AA-eclipsed pattern (orange line), AB-staggered pattern (purple line), and ABC-staggered pattern (blue line). Binding energies of  $\text{Cl}^-$  and  $^{99}\text{TcO}_4^-$  with SCU-COF-1. (f)  $\text{Cl}^-$  residence probability distribution within SCU-COF-1 in the control simulations (left) and the most preferential binding configuration of  $\text{Cl}^-$  to SCU-COF-1 (right top). The  $^{99}\text{TcO}_4^-$  binding configuration yielded by substituting  $\text{Cl}^-$  with  $^{99}\text{TcO}_4^-$  (right bottom). (g) Binding energies of  $\text{Cl}^-$  (green) and  $^{99}\text{TcO}_4^-$  (red) with SCU-COF-1 by computing their potential of mean force (PMF) profiles moving from their binding sites to the bulk water. The inset figure displays the reaction coordinate in the PMF calculation. Reproduced from ref 82. Copyright 2019, Royal Society of Chemistry.

ppm  $\text{TcO}_4^-$ . During these experiments, the adsorbent was agitated with the solution at 180 rpm, leading to an exceptionally rapid equilibrium achievement within 5 min. This quick equilibrium facilitated the successful capture of 98.2% of the  $\text{TcO}_4^-$ , highlighting the suitability of the sorbent for environmental remediation tasks. The efficiency and speed observed underscore the potential of 3DCOF-g-VBPPH<sub>3</sub>Cl for environmental remediation applications, especially in situations requiring prompt and effective removal of contaminants.<sup>79</sup>

While the efficient capture of  $\text{TcO}_4^-$  from natural water samples using COF materials shows promise, several advancements in COF technology have also been made for the recovery of  $\text{TcO}_4^-$  from nuclear-related wastes. One such example is the work by Yan and his team, who have developed a unique cationic COF, named DhaTG<sub>Cl</sub>, designed specifically for  $\text{TcO}_4^-$  capture. This material was synthesized using a Schiff reaction between triaminoguanidinium chloride (TG<sub>Cl</sub>) and 2,5-dihydroxyterephthalaldehyde (Dha). The novel DhaTG<sub>Cl</sub> material uniquely

combines cationic guanidine moieties with hydroxyl-anchored edge units and loosely bonded  $\text{Cl}^-$  ions within its porous structure. This distinctive design allows for rapid ion-exchange kinetics, which is especially effective for  $\text{ReO}_4^-$  adsorption, leading to an impressive sorption capacity of  $437 \text{ mg g}^{-1}$  and a remarkable  $K_d$  of  $5.0 \times 10^5 \text{ mL g}^{-1}$ . The blend of cationic sites, hydrogen bonding, and hydrophobic 1D channels embedded within  $\text{DhaTG}_{\text{Cl}}$  allows for the removal of  $\text{ReO}_4^-$  across a wide pH range (3–12). Interestingly, the material showcases selective capture of  $\text{ReO}_4^-$  even with excess of  $\text{NO}_3^-$ . It effectively removes roughly 73% of  $\text{ReO}_4^-$  from complex simulated Hanford LAW stream samples.<sup>80</sup> Similarly, Xia and his team have made strides in COF development through the synthesis of cationic guanidine-based COFs named TG-TPAL-H and TG-TPAL-OMe. These were created by coupling  $\text{TG}_{\text{Cl}}$  with terephthalaldehyde and 2,5-dimethoxyterephthalaldehyde, respectively. Notably, the electron-donating methoxy group present in TG-TPAL-OMe modifies the properties of the COF by decreasing the positive charge density of the guanidine groups. Thus, TG-TPAL-H demonstrates superior sorption efficiency compared to TG-TPAL-OMe, as evident by its increased uptake capacity ( $549$  vs.  $317 \text{ mg g}^{-1}$ ) and distribution coefficient ( $1.17 \times 10^6$  vs.  $6.9 \times 10^4 \text{ mL g}^{-1}$ ).<sup>81</sup>

Wang and his team have developed SCU-COF-1, a novel 2D viologen-based ionic COF. This COF is synthesized via the condensation of an aminated viologen with Tp, resulting in a material with standout features. These include ultra-high acid stability, resilience against high-dose irradiation, and exceptional  $^{99}\text{TcO}_4^-$  sorption capabilities, characterized by rapid sorption kinetics (equilibrium achieved within 1 min) and an extraordinary uptake capacity of  $702.4 \text{ mg g}^{-1}$  for  $\text{ReO}_4^-$ . SCU-COF-1 proves highly effective in separating  $^{99}\text{TcO}_4^-$  from both simulated highly acidic fuel reprocessing solutions (such as 3 M  $\text{HNO}_3$ ) and LAW streams from U.S. legacy nuclear sites. In specific tests, like in a simulated Hanford LAW melter recycle stream laden with high concentrations of  $\text{Cl}^-$ ,  $\text{NO}_2^-$ , and  $\text{NO}_3^-$ , which are at least 300 times more abundant than  $^{99}\text{TcO}_4^-$ , SCU-COF-1 demonstrated notable removal efficiencies: 20.9% at a phase ratio of 1, and 62.8% at a ratio of 5. Furthermore, under conditions simulating real used fuel reprocessing (253 ppm  $\text{ReO}_4^-$  in a 3 M  $\text{HNO}_3$  solution), SCU-COF-1 successfully removed 52.3% of  $\text{ReO}_4^-$  at a solid–liquid ratio of 1:40. These results highlight potential of SCU-COF-1 in  $^{99}\text{Tc}$  separation during early stages of used fuel reprocessing, even before the PUREX process (Figure 12).<sup>82</sup> In another development, Qiu and colleagues synthesized a 3D COF, named TFAM-BDNP, using the Zincke reaction. TFAM-BDNP is notable for its high adsorption capacity of  $998 \text{ mg g}^{-1}$  and a rapid-exchange kinetic rate of 60 s for  $\text{ReO}_4^-$ . The effectiveness of this material is ascribed to its hydrophobic channels, a plethora of binding sites, and high stability. Remarkably, TFAM-BDNP maintains strong adsorption performance for  $\text{ReO}_4^-$  even with a significant excess of competing anions, effectively functioning across a wide pH range from 2 to 12. In tests using simulated Hanford LAW samples, the 3D COF TFAM-BDNP displayed remarkable efficiency in removing  $\text{ReO}_4^-$ , achieving a 73% removal rate even when faced with a concentration of  $\text{SO}_4^{2-}$  that was 6000 times greater than that of  $\text{ReO}_4^-$ . This result underscores the robustness and effectiveness of TFAM-BDNP in handling challenging environmental conditions.<sup>83</sup> In parallel, Wang and his team introduced another innovative material, a 2D viologen COF named PS-COF-1. This COF was synthesized by condensing 1,1'-bis(4-formylphenyl)-4,4'-bipyridinium with

1,3,5-tris(4-aminophenyl)benzene. PS-COF-1 stands out due to its exceptionally high BET area of  $2703 \text{ m}^2 \text{ g}^{-1}$  and a pore size of 4.5 nm, which contribute to its impressive adsorption capacity of  $1262 \text{ mg g}^{-1}$ . A significant feature of PS-COF-1 is its capability to rapidly purify  $\text{ReO}_4^-/^{99}\text{TcO}_4^-$  contaminated potable water, reducing concentrations from 10 ppb to 1 ppm to safe drinking water levels within 10 min. This demonstrates the potential of PS-COF-1 for use in water purification applications, addressing critical environmental and health concerns.<sup>84</sup>

Du and collaborators developed a composite material, bis- $\text{PC}_6@$ TbDp-COF, using a host–guest assembly method. This process involved in-situ polymerizing vinyl-functionalized ionic monomers within the pore channels of a COF. The material displayed remarkable efficiency in removing  $\text{ReO}_4^-$ , achieving 93% removal at a phase ratio of 20  $\text{g L}^{-1}$  from a 1 M NaOH solution and an adsorption capacity of  $2.33 \text{ mg g}^{-1}$ . Increasing the solid/liquid ratio to 40 enhanced the removal efficiency to 96% in the highly alkaline solution, though the uptake capacity dropped to  $1.20 \text{ mg g}^{-1}$ . The researchers then tested bis- $\text{PC}_6@$ TbDp-COF in a simulated stream mimicking the SRS HLW, which contains high levels of various ions and  $7.92 \times 10^{-5} \text{ M TcO}_4^-$ . In this complex mixture, bis- $\text{PC}_6@$ TbDp-COF retained about 33% of its  $\text{ReO}_4^-$  removal capacity at a phase ratio of 40, but its uptake capacity decreased due to the nucleophilic attacks on some imidazolium groups within the material by  $\text{OH}^-$  ions in the SRS stream.<sup>85</sup>

In another study, Qiu and colleagues created an innovative olefin-linked cationic COF, BDBI-TMT, by condensing 2,4,6-trimethyl-1,3,5-triazine (TMT) with 5,6-bis(4-formylbenzyl)-1,3-dimethylbenzimidazolium bromide (BDBI). This material demonstrated exceptional stability under various extreme conditions. It maintained its PXRD patterns and infrared (IR) spectra even after exposure to 6.0 M NaOH, HCl, or  $\text{HNO}_3$  and 600 kGy of  $\beta$ - and  $\gamma$ -ray irradiation for 3 days. The impressive efficiency of BDBI-TMT in ion exchange with  $\text{ReO}_4^-$ , resulting in a capacity of  $726 \text{ mg g}^{-1}$ , can be attributed largely to the abundant and meticulously designed imidazolium moieties strategically positioned on the highly accessible pore walls. The introduction of a highly conjugated, bulky alkyl structure into the framework enhances both its hydrophobicity and chemical stability. This structural innovation significantly increases the affinity of BDBI-TMT for  $\text{ReO}_4^-/\text{TcO}_4^-$ , enabling selective and reversible adsorption of these radioactive ions under harsh conditions. In a simulated Hanford LAW stream, containing,  $\text{NO}_2^-$ ,  $\text{NO}_3^-$ , and  $\text{Cl}^-$  at concentrations over 300-fold greater than  $\text{TcO}_4^-$ , BDBI-TMT showed remarkable efficiency. Under comparable experimental conditions, BDBI-TMT was able to remove 89.1% of  $\text{ReO}_4^-$  from the waste at a phase ratio of 5, demonstrating its potential for effective radioactive waste management.<sup>86</sup>

Additionally, the research team pioneered an innovative approach to fabricate ionic 3D  $\text{sp}^2$  carbon-linked COFs, specifically known as TAPM-PZI and TFPM-PZI. This method entailed an acid-catalyzed Aldol condensation process between 1,2,5-trimethylpyrazin-1-ium iodide (PZI) and tetra(4-formylphenyl)methane (TFPM) or 1,3,5,7-tetrakis(4-aldophenyl)adamantane (TAPM), respectively. Both COFs exhibited classic type I isotherms, confirming their microporous nature, with BET surface areas of  $598.3 \text{ m}^2 \text{ g}^{-1}$  for TAPM-PZI and  $501.6 \text{ m}^2 \text{ g}^{-1}$  for TFPM-PZI. They showed exceptional chemical stability, maintaining crystallinity even in extreme conditions of 6 M NaOH and 6 M HCl. The unique, highly

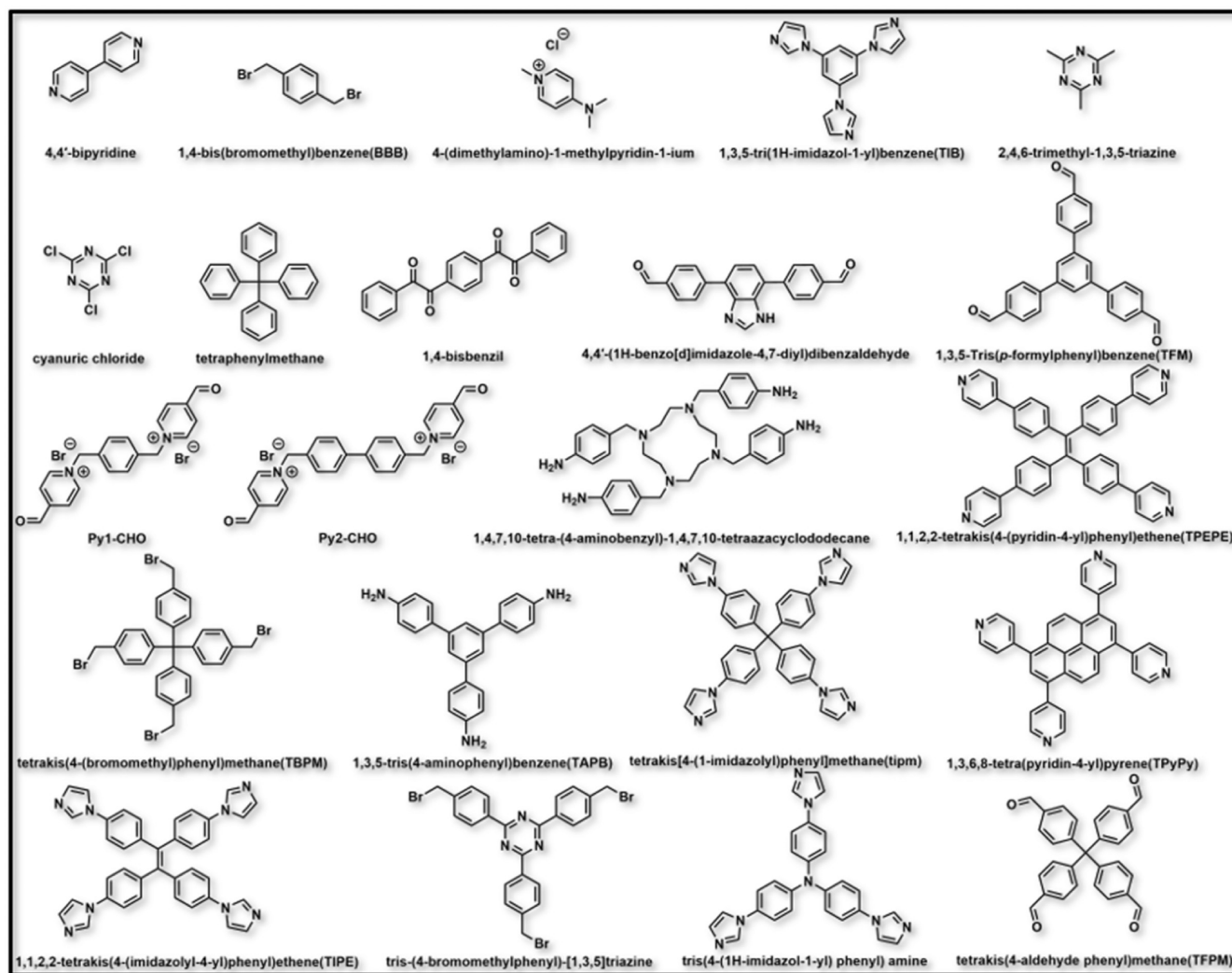


**Figure 13.** Molecular structures of the monomers used in constructing the POPs discussed in this Review.

symmetrical 3D building blocks in these COFs distribute positive charges evenly, making them highly effective for the rapid removal of  $\text{ReO}_4^-/\text{TcO}_4^-$ . Specifically, TFPM-PZI in its chloride form (TFPM-PZ-Cl), achieved through ion exchange from  $\text{I}^-$  to  $\text{Cl}^-$ , displayed a notable adsorption capacity of  $542.3 \text{ mg g}^{-1}$ . In a simulated Hanford LAW scrubber solution, TFPM-PZ-Cl displayed an impressive 86.4% removal efficiency for  $\text{ReO}_4^-$  at a phase ratio of  $5 \text{ mg mL}^{-1}$ . Remarkably, after undergoing column adsorption, the  $\text{ReO}_4^-$  concentration in the solution was dropped to approximately 10 ppb, achieving an exceptional 99.99% removal rate. This performance highlights TFPM-PZ-Cl as a highly efficient material for extracting  $\text{ReO}_4^-/\text{TcO}_4^-$  from industrial wastewater, showcasing its potential for practical applications in waste management.<sup>87</sup>

In another significant advancement, the research team developed an ionic COF characterized by an extremely rapid fluorescence response (within 2 s) and outstanding selectivity toward  $\text{ReO}_4^-$ . This COF was fabricated through the condensation of Tp and 3,3'-dihydroxybenzidine and subsequently modified postsynthetically with (2-bromoethyl)-trimethylammonium bromide. The fast adsorption kinetics of this material can be ascribed to several key factors. Firstly, its abundant ionic sites facilitate efficient interactions with  $\text{ReO}_4^-$ . Additionally, the COF features regular hydrophobic pore

channels that accelerate the rapid diffusion and adsorption of target ions. Moreover, enhanced intramolecular charge transfer in the material boosts its adsorption capabilities and selectivity. The adsorption kinetics of this ionic COF are particularly notable, achieving equilibrium in 3 min. This rapid attainment of equilibrium, combined with a high adsorption capacity of  $439 \text{ mg g}^{-1}$  and a low detection limit of  $1.04 \text{ }\mu\text{M}$ , underscores the potential of this material for the detection and removal of  $^{99}\text{TcO}_4^-/\text{ReO}_4^-$  under realistic conditions. Overall, the ultrafast fluorescence response, exceptional selectivity, and impressive adsorption properties of this ionic COF suggest its significant potential for applications in the detection and recovery of  $^{99}\text{TcO}_4^-/\text{ReO}_4^-$  in various real-world scenarios.<sup>88</sup>

## ■ AMORPHOUS POP-BASED SORBENTS

The programming of structure and composition in materials is not limited to ordered crystalline solids; it is also achievable in various amorphous porous polymers through a modular approach. In some instances, the characteristics of these materials are primarily determined by their molecular repeat units, allowing for the functional programming of these materials without necessitating long-range structural order. POPs are a notable example of such materials. They are a diverse class of multidimensional porous organic materials, formed through

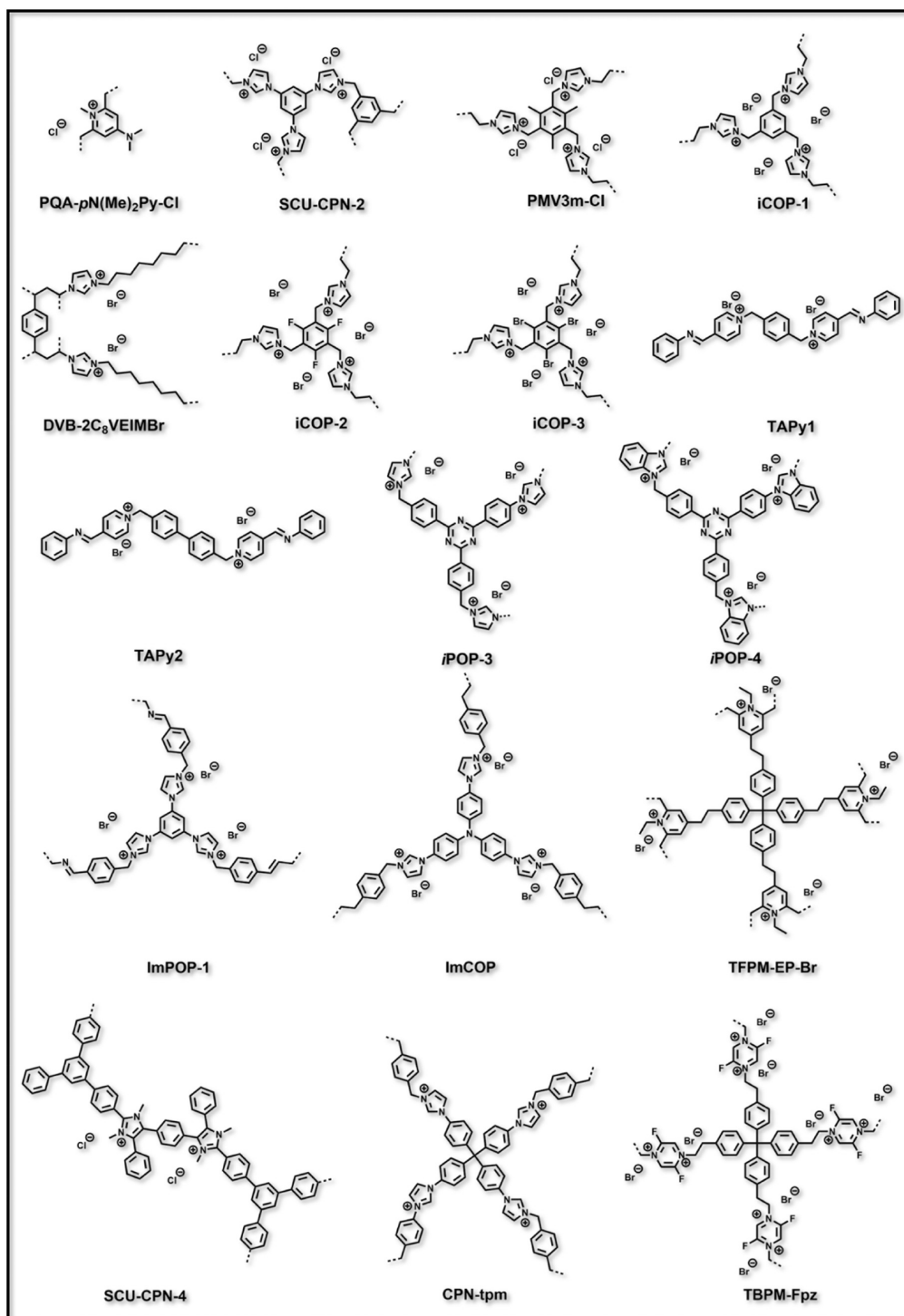
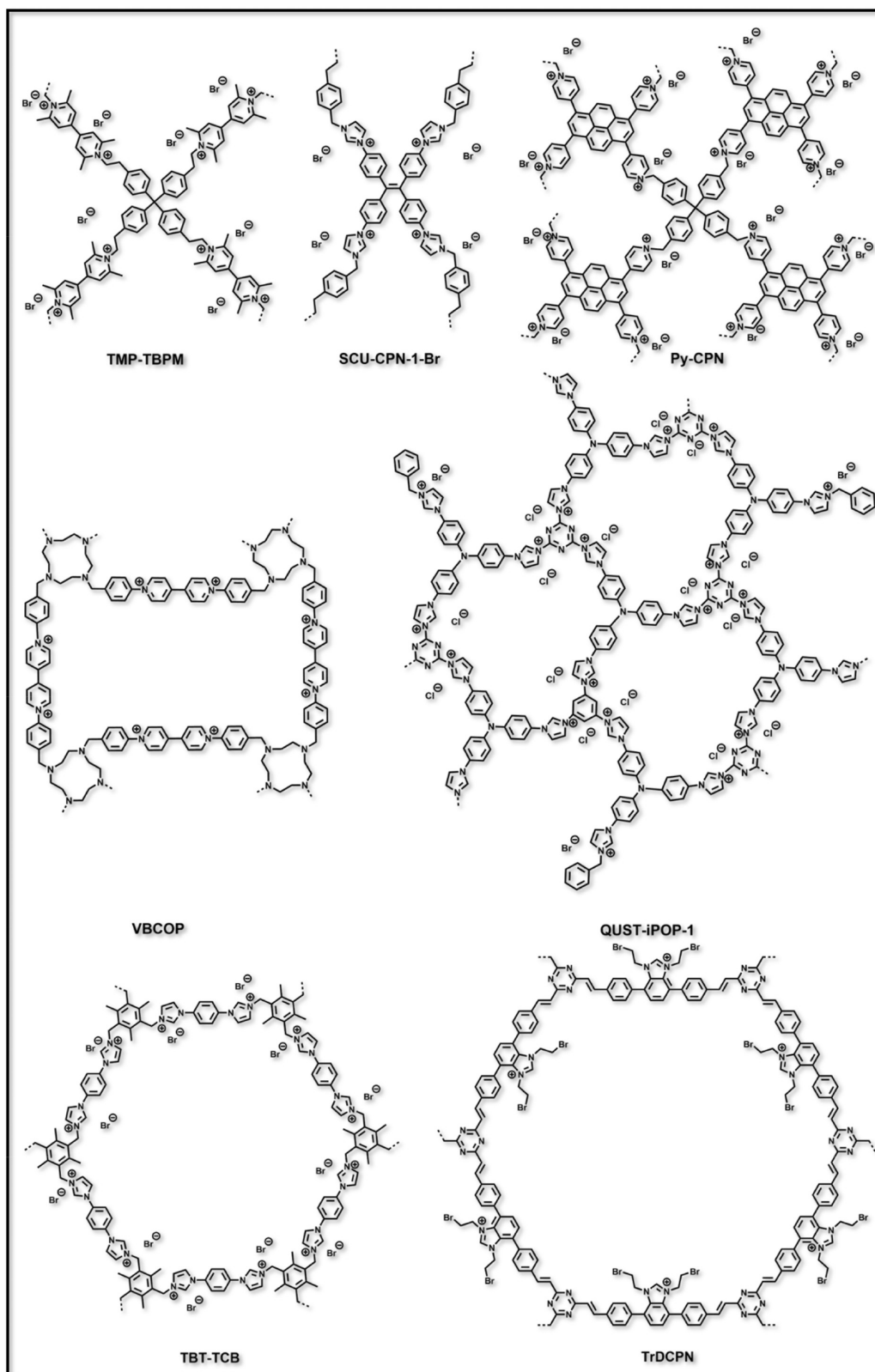


Figure 14. continued



**Figure 14.** Chemical structures of the POPs discussed in this Review.

robust covalent bonds between a variety of organic building blocks. These building blocks differ in geometry and topology, making POPs an increasingly researched and versatile class of porous materials. POPs share similarities with MOFs in several aspects, such as their predictable synthesis, customizable pore

features, and capability to target specific environmental pollutants. A distinctive advantage of POPs over many MOFs is their exceptional hydrolytic stability, even under extremely acidic or basic conditions. The molecular structures of the monomers used in constructing the POPs and the structures of



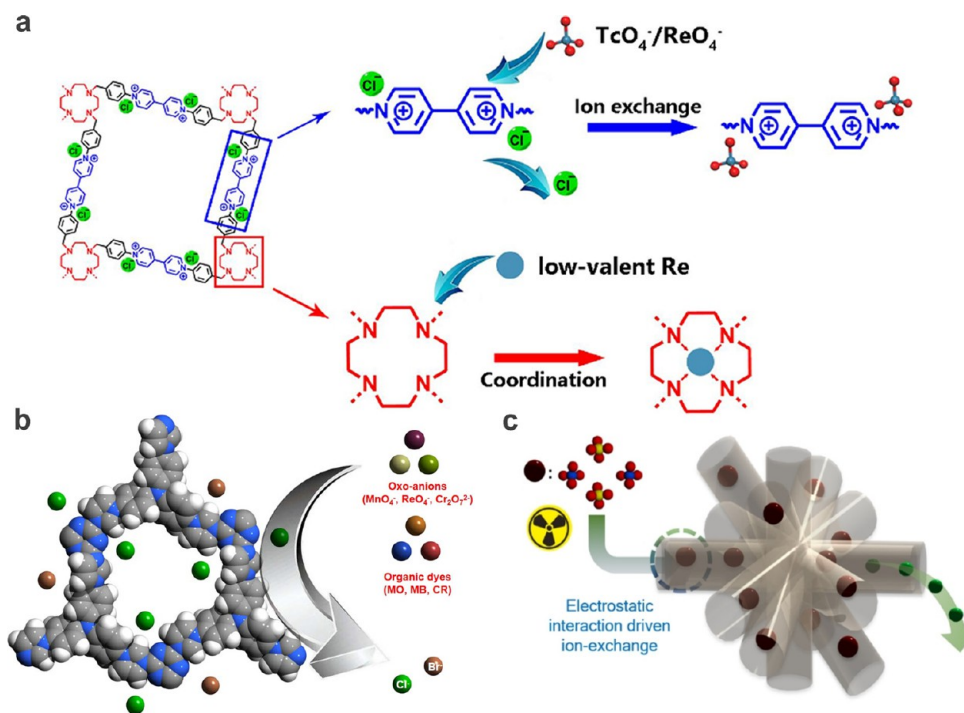


**Figure 15.** (a) Adsorption mechanism of VBCOP toward Tc/Re(VII) and low-valent Re. Reproduced from ref 92. Copyright 2019, Elsevier. (b) Space-filling view of QUST-iPOP-1 in an amorphous periodic cell and schematic of the oxo-anions and organic dye capture (gray, C; white, H; blue, N; green, Cl; brown, Br). Reproduced from ref 95. Copyright 2021, American Chemical Society. (c) Schematic representation of toxic oxo-anion capture in iPOPs. Reproduced from ref 97. Copyright 2021, John Wiley and Sons.

the resulting POPs discussed in this Review are illustrated in Figures 13 and 14.

Wang and team have made significant strides in this field with the introduction of SCU-CPN-1-Br, a cationic porous organic polymer. This polymer is synthesized by quaternizing 1,4-bis(bromomethyl)benzene (BBB) with 1,1,2,2-tetrakis(4-(imidazolyl-4-yl)phenyl)ethene (TIPE). A notable feature of SCU-CPN-1-Br is its remarkable resilience to high-energy ionizing radiation, making it a prime candidate for applications in nuclear fuel reprocessing and waste management. Remarkably, SCU-CPN-1-Br retains its sorption capacity of 876 mg  $\text{ReO}_4^-$  per gram even after exposure to 1000 kGy of  $\beta$ - or  $\gamma$ -rays. This is in stark contrast to conventional commercial resins, which show a 30% reduction in sorption capacity under similar conditions, thereby underscoring their limitations in handling used nuclear fuel. In specific experiments aimed at isolating  $\text{ReO}_4^-$  from a 3 M  $\text{HNO}_3$  solution, SCU-CPN-1-Br demonstrated its efficacy. At a phase ratio of 20, it was able to remove around 40% of  $\text{ReO}_4^-$ , and at a ratio of 90, comparable to the conditions in a chromatographic column, it achieved a removal rate of 76% of the available  $\text{ReO}_4^-$ . This performance highlights the potential of SCU-CPN-1-Br in practical applications related to environmental remediation and nuclear waste management. This underscores the preference of SCU-CPN-1-Br for  $\text{ReO}_4^-/\text{TcO}_4^-$  over  $\text{NO}_3^-$ , a critical aspect in eliminating  $\text{TcO}_4^-$  from reprocessed used nuclear fuel prior to the PUREX process. SCU-CPN-1 demonstrated a remarkable ability to selectively capture  $\text{TcO}_4^-$  in the Hanford LAW stream. Specifically, at a solid/liquid ratio of 5, it successfully sequestered nearly 90% of the available  $\text{TcO}_4^-$  from the waste. This impressive performance underscores the potential of SCU-CPN-1 in nuclear industry applications.<sup>89</sup>

In environments with high ion concentrations, particularly in the context of removing  $\text{TcO}_4^-$  from groundwater sources and legacy tank waste, the sorbents must possess a high enthalpy of adsorption specific to  $\text{TcO}_4^-$ . A strategy that integrates multiple cooperative functionalities within a single material has proven effective in ensuring high affinity. Ma et al. tackled this challenge by designing porous adsorbent materials made entirely of functional moieties, thereby maximizing the density of accessible anion-exchange sites in the nanotraps. This research, utilizing pyridinium as the cationic building unit, demonstrated that modifying the local environment around the positive site significantly enhances its affinity for  $\text{TcO}_4^-$ . These materials showed excellent radiation resistance and chemical stability, making them suitable for diverse challenging conditions. One particularly effective material, PQA-*p*N(Me)<sub>2</sub>Py-Cl, featuring 4-(dimethylamino)-1-methylpyridin-1-ium chloride moieties, showcased an impressive  $\text{ReO}_4^-$  sorption capacity of 1127 mg  $\text{g}^{-1}$ . It demonstrated unparalleled extraction efficiency in scenarios relevant to used fuel reprocessing and legacy nuclear wastes. For instance, PQA-*p*N(Me)<sub>2</sub>Py-Cl extracted ~70% of  $\text{ReO}_4^-$  from an  $\text{HNO}_3$  aqueous solution with a molar ratio of  $\text{NO}_3^-/\text{ReO}_4^-$  of 1875 at a solid/liquid ratio of 50 mL  $\text{g}^{-1}$ . At a reduced phase ratio of 20 mL  $\text{g}^{-1}$ , it removed 90% of  $\text{ReO}_4^-$ . This material also exhibited selective extraction of  $\text{TcO}_4^-$  from simulated Hanford LAW streams. At a phase ratio of 200 mL  $\text{g}^{-1}$ , PQA-*p*N(Me)<sub>2</sub>Py-Cl efficiently separated ~95% of  $\text{TcO}_4^-$ . The potential of PQA-*p*N(Me)<sub>2</sub>Py-Cl for decontaminating  $\text{TcO}_4^-$  at the SRS, where the solution is highly basic, and  $\text{TcO}_4^-$  is outnumbered by other anions by over 70,000 times, was also investigated. The experiment revealed that at a phase ratio of 100 mL  $\text{g}^{-1}$ , PQA-*p*N(Me)<sub>2</sub>Py-Cl successfully extracted approximately 80% of available  $\text{TcO}_4^-$ . This level of selectivity is unmatched in current studies, underscoring its potential for

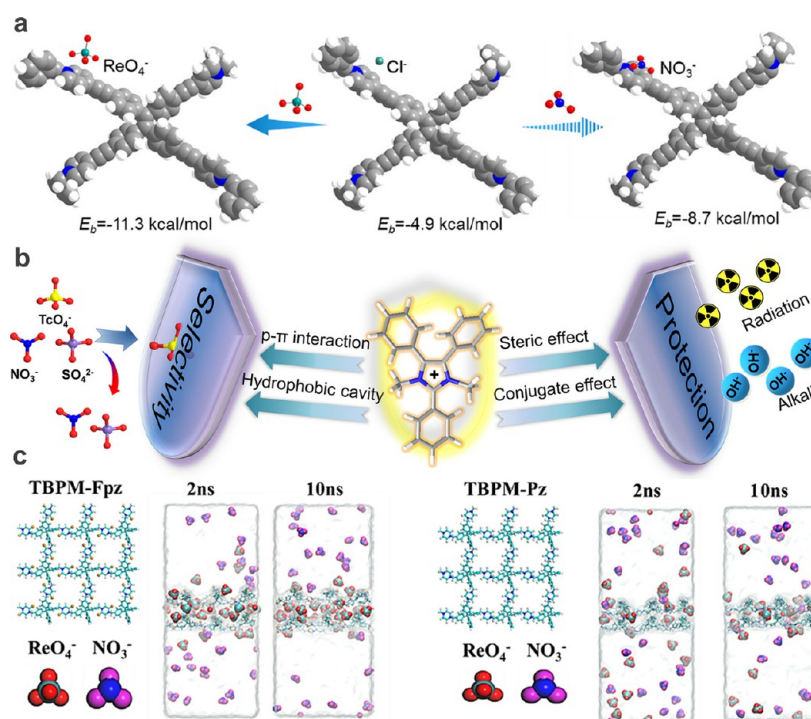


**Figure 16.** (a) Optimized sorption geometries of  $[\text{M1}]^+$  with  $\text{ReO}_4^-$ ,  $\text{NO}_3^-$ , and  $\text{Cl}^-$ . Reproduced from ref 99. Copyright 2022, American Chemical Society. (b) Illustration of designing the cationic key structural fragment of a task-specific CPNs. Reproduced from ref 104. Copyright 2021, American Chemical Society. (c) Adsorption kinetics simulation of  $\text{ReO}_4^-$ . Time series snapshot showing the adsorption process in TBPM-Fpz and TBPM-Pz. Reproduced from ref 108. Copyright 2023, Elsevier.

practical use in nuclear waste cleanup. The exceptional performance of PQA-*p*N(Me)<sub>2</sub>Py-Cl is primarily attributed to the electron-donating properties of the dimethylamino group, which promotes the formation of kinetically labile complexes, enhancing rapid ion exchange. This discovery holds significance, as ion-exchange mechanisms are often consistent across different sequestration processes, suggesting the broader applicability of these findings.<sup>90</sup>

In parallel work, Han and their team developed ImPOP-1, a cationic porous polymer based on imidazolium. Their research used  $\text{ReO}_4^-$  and recorded an adsorption capacity of 610  $\text{mg g}^{-1}$  for  $\text{ReO}_4^-$ .<sup>91</sup> Another notable study by Xia and colleagues describes a viologen-based cationic polymer (VBCOP), synthesized via the Zincke reaction involving 1,4,7,10-tetra(4-aminobenzyl)-1,4,7,10-tetraazacyclododecane and 4,4'-bipyridine. Its design features numerous anion-exchange sites provided by viologen groups, effective for  $\text{TcO}_4^-/\text{ReO}_4^-$  adsorption. The incorporation of flexible tetraaza macrocycle knots in the polymer is thought to form coordinate complexes with low-valent Tc/Re, facilitating adsorption primarily through ion exchange. Furthermore, the inclusion of a flexible tetraaza macrocycle ligand in VBCOP boosts its capacity for capturing  $\text{ReO}_4^-$ . VBCOP, therefore, shows potential for remediating different valent of Tc species in nuclear wastewater treatment (Figure 15a).<sup>92</sup>

In 2021, Wang and their team developed a novel cationic polymer network material, SCU-CPN-2, through a detailed process involving precursor screening and structure prediction. SCU-CPN-2, synthesized using 1,3,5-tri(1*H*-imidazol-1-yl)benzene (TIB) and BBB, stands out for its high positive charge density and excellent radiation resistance. It demonstrates an exceptional adsorption capacity for  $\text{ReO}_4^-$ , reaching 1,467  $\text{mg g}^{-1}$ , surpassing all previously known anion-exchange materials.

Additionally, SCU-CPN-2 exhibits ultrafast adsorption kinetics, high selectivity against  $\text{NO}_3^-$  and  $\text{SO}_4^{2-}$ , and ease of recyclability, making it a highly effective material for removing contaminants from nuclear waste streams.<sup>93</sup> Concurrently, Ma and colleagues created an imidazole-based cationic polymer, CPN-tpm, by reacting tetrakis[4-(1-imidazolyl)phenyl]methane (tipm) with 1,4-bis(bromomethyl)benzene. This material demonstrated an impressive  $\text{ReO}_4^-$  adsorption rate of 1,133  $\text{mg g}^{-1}$ .<sup>94</sup> In another study, Ma et al. synthesized QUST-iPOP-1, an imidazolium-based cationic porous polymer, through a two-step quaternization process using tris(4-imidazolylphenyl)amine and cyanuric chloride, followed by benzyl bromide. QUST-iPOP-1 exhibited an uptake capacity for  $\text{ReO}_4^-$  of 441.6  $\text{mg g}^{-1}$  (Figure 15b).<sup>95</sup> Lou and their team reported on DVB-2C<sub>8</sub>VEIMBr, an imidazolium-based ionic liquid polymer. Created through the copolymerization of divinylbenzene with an imidazolium-based ionic monomer, it showed a  $\text{ReO}_4^-$  uptake capacity of 313  $\text{mg g}^{-1}$ . These studies collectively contribute significant advancements in materials for nuclear waste remediation.<sup>96</sup> Ghosh described the synthesis of two imidazolium-functionalized ionic porous polymers, iPOP-3 and iPOP-4. These were created by a quaternization reaction between tris(4-bromomethylphenyl)[1,3,5]triazine and either imidazole or benzimidazole. They exhibited  $\text{ReO}_4^-$  adsorption capacities of 515.5 and 350.3  $\text{mg g}^{-1}$ , respectively (Figure 15c).<sup>97</sup> Qiu et al. synthesized an imidazolium-based cationic organic polymer (named ImCOP), via the quaternization reaction between tris(4-(1*H*-imidazol-1-yl)phenyl)amine and 1,4-bis(bromomethyl)benzene to form a semirigid structure for efficient adsorption of  $\text{ReO}_4^-$ , affording a  $\text{ReO}_4^-$  uptake capacity of 1162  $\text{mg g}^{-1}$ .<sup>98</sup> In a parallel study, Xiao and colleagues reported the creation of a similar pyridium cationic network using tetrakis(4-(4-(pyridyl)ethynyl)phenyl)ethene

(TPEPE) and BBB, exhibiting an impressive  $\text{ReO}_4^-$  adsorption capacity of  $813 \text{ mg g}^{-1}$ , emphasizing its potential for contamination clean-up applications (Figure 16a).<sup>99</sup> Wang and their team introduced a straightforward method to create an imidazolium-based cationic polymer, PMV3m-Cl. Utilizing free radical polymerization of a vinyl-functionalized tri-imidazolium-charged monomer, they achieved a  $\text{ReO}_4^-$  adsorption capacity of  $739 \text{ mg g}^{-1}$ .<sup>100</sup>

In 2023, Ma and their team developed a proactive approach to synthesize two types of cationic POPs with self-adaptive capabilities for the removal of  $^{99}\text{TcO}_4^-/\text{ReO}_4^-$  from water. This innovative method leveraged single-crystal structures and was informed by the known affinity of two pyridinium compounds, Py1 and Py2, for  $^{99}\text{TcO}_4^-/\text{ReO}_4^-$ . By growing single crystals, they were able to refine their approach. The team introduced aldehyde groups into Py1 and Py2, creating Py1-CHO and Py2-CHO. These compounds were then reacted with 1,3,5-tris(4-aminophenyl)benzene (TAPB) to form layered cationic POPs, TAPy1 and TAPy2. The resulting materials showed high adsorption capacities: TAPy1 at  $399 \text{ mg g}^{-1}$  and TAPy2 at  $309 \text{ mg g}^{-1}$ . Notably, they were extremely efficient in removing radioactive  $^{99}\text{TcO}_4^-$ , with a 97% removal rate achieved in 30 s. A detailed investigation into the adsorption mechanism, using single-crystal X-ray analysis and DFT calculations, revealed that the host–guest interaction observed in single crystals plays a crucial role in determining the structure and properties of these materials.<sup>101</sup>

Qiu and colleagues developed a groundbreaking 3D olefin-linked ionic conjugated microporous polymer named TFPM-EP-Br, synthesized using tetrakis(4-aldehyde phenyl)methane (TFPM) as the core monomer. This polymer stands out for its unique cationic cavity and hydrophobic structure, qualities that render it an efficient fluorescent sensor for  $\text{TcO}_4^-$ . The sensing mechanism is based on electron transfer from TFPM-EP-Br to  $\text{TcO}_4^-$ , leading to the formation of nonfluorescent complexes that effectively quench the fluorescence of the polymer. This property provides a novel method for detecting this radioactive ion. Additionally, the well-defined pore channels in the polymer structure are crucial in facilitating rapid mass transfer of  $\text{TcO}_4^-$ , contributing to an ultrafast response time of less than 2 s and a remarkably low detection limit of 33.3 nM. Furthermore, TFPM-EP-Br demonstrates a significant adsorption capacity for  $\text{TcO}_4^-$ , reaching up to  $346 \text{ mg g}^{-1}$ .<sup>102</sup> Expanding on their innovative approaches, the same research group developed a porous polymer named Py-CPN using a nucleophilic substitution reaction. This process involved reacting tetrakis(4-(bromomethyl)phenyl)methane (TBPM), a 3D building unit, with 1,3,6,8-tetra(pyridin-4-yl)pyrene (TPyPy). The tetrahedral unit of TBPM inherent rigidity and shape persistence facilitate rapid ion transportation throughout the polymeric network. As a result, Py-CPN exhibits an impressive adsorption capacity of  $513.7 \text{ mg g}^{-1}$  and fast kinetics for  $\text{ReO}_4^-$  removal, effectively eliminating it in a minute. The inclusion of TPyPy, a highly hydrophobic and extensively conjugated monomer, endows Py-CPN with remarkable selectivity against various coexisting anions. Additionally, Py-CPN maintains stable sorption capabilities over a wide pH range, including in 3 M  $\text{HNO}_3$  solution and simulated Hanford LAW. At a phase ratio of 20, the removal rate for these contaminants is 28.8%, which increases to 58.2% when the ratio is raised to 40.<sup>103</sup>

Wang and colleagues devised an innovative approach to enhance the alkaline resistance of sorbents, hypothesizing that the addition of bulky groups at strategic positions of the

imidazolium moiety could shield against nucleophilic attacks from  $\text{OH}^-$ . This could prove advantageous for managing alkaline nuclear waste. Building on this idea, they developed a novel alkaline-stable imidazolium-based polymer, SCU-CPN-4, by introducing bulky alkyl groups at the N1, C2, N3, C4, and C5 positions of the imidazolium unit. The synthesis process involved the condensation of 1,4-bisbenzil and 1,3,5-tris(*p*-formylphenyl)benzene (TFP), followed by quaternization with methyl iodide. SCU-CPN-4 exhibits the beneficial characteristics of previously reported cationic CPNs in removing  $^{99}\text{TcO}_4^-$ , such as high  $^{99}\text{TcO}_4^-$  uptake capacity, rapid sorption kinetics, excellent selectivity, and superior radiation resistance. Crucially, SCU-CPN-4 overcomes the issue of poor alkaline stability, fulfilling the criteria for remediating  $^{99}\text{TcO}_4^-$  in actual alkaline nuclear waste environments. In simulated SRS waste, SCU-CPN-4 demonstrated a high removal efficiency of  $\text{TcO}_4^-$ , achieving 94.3% at a phase ratio of 20  $\text{g L}^{-1}$ . Further reinforcing its application in real scenario, SCU-CPN-4 maintained consistent  $\text{ReO}_4^-$  removal efficiency for at least four cycles in simulated SRS waste streams. Column sorption tests using SCU-CPN-4 in a simulated SRS HLW stream were particularly telling, as demonstrated by the fact that 300 mg of SCU-CPN-4 was able to effectively remove nearly all  $\text{ReO}_4^-$  from the first 40 mL of the SRS HLW waste solution, demonstrating its high initial removal efficiency for  $\text{ReO}_4^-$ . These findings highlight the exceptional structural stability and excellent sorption selectivity of SCU-CPN-4, indicating its potential for direct application in the elimination of  $\text{TcO}_4^-$  from highly alkaline streams, such as those encountered at the SRS (Figure 16b).<sup>104</sup>

Wang et al. developed a groundbreaking series of ionic polymers, which incorporate imidazolium sites serving as nanotraps for binding  $^{99}\text{TcO}_4^-$ . Modifications were made to the base polymer, iCOP-1, including substitutions of C–H species on the benzene ring near the imidazolium- $\text{N}^+$  sites with either fluorine (transforming it into iCOP-2) or bromine (creating iCOP-3), greatly enhancing its binding affinity and offering insight into crucial structure–property correlations. Impressively, these polymers demonstrated high adsorption capacities. iCOP-1 had a capacity of  $1434 \text{ mg g}^{-1}$ , while iCOP-2 and iCOP-3 manifested capacities of 765 and  $778 \text{ mg g}^{-1}$ , respectively. Particularly noteworthy is that iCOP-1 showcased superior ability in removing  $^{99}\text{TcO}_4^-/\text{ReO}_4^-$  from contaminated tap water and groundwater dynamically and efficiently, surpassing the performance of commercial ion-exchange resins, besides other reported materials. The innovative iCOP-2 polymer, with the integration of C–F bonds into its structure, demonstrated a substantial increase in hydrophobicity and a decrease in polarity. This change successfully curbed the affinity of  $\text{H}^+$  and  $\text{NO}_3^-$  toward the imidazolium moieties, enhancing the selectivity for  $^{99}\text{TcO}_4^-$  adsorption, even under strongly acidic conditions. In practical tests, iCOP-2 managed to eliminate more than 58% of  $\text{ReO}_4^-$  from a 3 M  $\text{HNO}_3$  solution with 28 ppm of  $\text{ReO}_4^-$ , using a phase ratio of 60  $\text{g L}^{-1}$ . Adding to the advancement, iCOP-3 polymer integrated bromine groups onto the aromatic linkers, amplifying its hydrophobicity and introducing strong steric hindrances at the imidazolium- $\text{N}^+$  binding sites. This adjustment increased its binding affinity and selectivity. Additionally, these adjustments made iCOP-3 remarkably effective at the preferential adsorption of  $^{99}\text{TcO}_4^-$  under highly alkaline conditions, as witnessed in 3 M NaOH solutions. Significantly, iCOP-3 demonstrated high efficiency (>85% removal) in extracting  $^{99}\text{TcO}_4^-$  from solutions representative of the LAW streams at Hanford and other US

legacy nuclear sites. This suggests its potential applicability in remediating nuclear waste contaminants under diverse and challenging environmental conditions.<sup>105</sup>

In their innovative research, Qiu and colleagues achieved a significant breakthrough by integrating bulky methyl groups near the imidazole units in TBT-TCB. This strategic addition substantially enhanced the base resistance of the material. The structural modification introduced steric and electronic effects that effectively inhibited OH<sup>-</sup>-induced ring-opening reactions in the imidazole units. As a result, the modified TBT-TCB exhibited an impressive 85% removal efficiency for ReO<sub>4</sub><sup>-</sup> in a 1 M NaOH environment. Furthermore, the integration of methyl groups into TBT-TCB not only increased its hydrophobic properties but also improved its affinity for the hydrophobic and larger <sup>99</sup>TcO<sub>4</sub><sup>-</sup> ion. This enhancement allowed TBT-TCB to maintain high removal efficiency, even in environments with competitive ions, achieving an 84% removal rate in a 1 M H<sub>2</sub>SO<sub>4</sub> setting.<sup>106</sup> Following this, the research group skillfully developed a donor–acceptor (D-A) cationic polymeric framework named TrDCPN. This framework was designed with halogens to effectively extract ReO<sub>4</sub><sup>-</sup> from water. A hydrophobic network was synthesized through the combination of a donor molecule, 4,4'-(1*H*-benzo[*d*]imidazole-4,7-diyl)dibenzaldehyde, and an acceptor, 2,4,6-trimethyl-1,3,5-triazine. The introduction of halogen recognition sites through 1,2-dibromoethane enhanced the functionality of the network. Characterized by its extensive conjugated modules, a triazine core, and hydrophobic chains, this material displayed remarkable properties, including hydrolytic stability in extreme pH conditions of 3 M NaOH or 5 M HNO<sub>3</sub> and exceptional selectivity ( $K_d = 1.15 \times 10^4$  mL g<sup>-1</sup>). To illustrate the importance of the halogen  $\delta$ -hole interaction with ReO<sub>4</sub><sup>-</sup>, a comparative cationic polymer, TrECPN, lacking halogens, was synthesized. As expected, TrDCPN showed a superior uptake capacity of 420.3 mg g<sup>-1</sup>, significantly outperforming the uptake capacity of TrECPN of 283.6 mg g<sup>-1</sup>.<sup>107</sup>

Zhang and team made a significant advancement by creating a 3D fluorinated pyrazinium-based cationic polymer, TBPM-Fpz. This polymer is specifically engineered for rapid and selective extraction of ReO<sub>4</sub><sup>-</sup>, thanks to its high charge density. Its synthesis incorporates tetraphenylmethane as the structural building block and fluorinated pyrazine as a linker. This design endows TBPM-Fpz with both high charge and relative hydrophobicity. TBPM-Fpz stands out for its rapid sorption kinetics, reaching equilibrium in 3 min, and exhibits a remarkable sorption capacity of 833 mg g<sup>-1</sup>. Its selectivity for ReO<sub>4</sub><sup>-</sup> is also notable, achieving 92% even with a 1000-fold excess of SO<sub>4</sub><sup>2-</sup>. In simulated environments, TBPM-Fpz proved exceptionally effective, removing 95% of ReO<sub>4</sub><sup>-</sup> in the SRS HLW stream at a phase ratio of 40:1, and 89.8% in Hanford LAW wastewater at a 1:1 ratio. The outstanding performance of TBPM-Fpz is attributed to the fluorination process, which not only enhances its charge density but also minimizes steric hindrance. This research highlights the significant potential of fluorinated ionic polymers in efficiently removing ReO<sub>4</sub><sup>-</sup> from strongly alkaline wastewater. Additionally, it offers valuable insights into the strategic design of efficient cationic polymers for the treatment of TcO<sub>4</sub><sup>-</sup> in the alkaline nuclear waste (Figure 16c).<sup>108</sup>

Cui and colleagues achieved a breakthrough with the development of TMP-TBPM, an ultra-stable 3D pyridinium-based network. This material is particularly notable for its exceptional resilience to radiation, acids, and bases, making it

ideal for selectively capturing ReO<sub>4</sub><sup>-</sup>. Its hydrophobic design and reliance on steric hindrance are key to its robustness. It withstands exposure to 6 M HNO<sub>3</sub> and 6 M NaOH solutions, as well as significant doses of  $\gamma$ -rays (100, 200, and 600 kGy) and  $\beta$ -rays (100, 200, and 600 kGy). In batch capture experiments, TMP-TBPM demonstrated a high capture capacity of 918.7 mg g<sup>-1</sup> and rapid sorption kinetics, achieving 94.3% removal of ReO<sub>4</sub><sup>-</sup> in 2 min. The effectiveness of TMP-TBPM is attributed to its dense distribution of pyridinium moieties within highly accessible 3D pore channels. The inclusion of alkyl and tetraphenylmethane moieties significantly enhances the hydrophobicity and stability of the network. This not only increases its affinity toward <sup>99</sup>TcO<sub>4</sub><sup>-</sup>/ReO<sub>4</sub><sup>-</sup> but also enables selective and reversible capture of these isotopes, even in highly alkaline conditions. These findings underscore the promising potential of TMP-TBPM for advanced applications, particularly in selective capture under challenging environmental conditions.<sup>109</sup>

## CONCLUSION

The revival of interest in the extraction of TcO<sub>4</sub><sup>-</sup> from nuclear waste and from environmental sources can be linked to the projected increase in the use of nuclear power as a sustainable, low-carbon baseline energy source. Techniques for this extraction have continuously advanced since the inception of this field, ranging from solvent extraction, incorporation of inorganic materials, ion-exchange resins, to the latest approaches involving nanostructured materials, MOFs, COFs, and POPs. Over the past five years, sophisticated adsorbents have showcased a massive improvement in adsorption capabilities, surpassing the traditional adsorbents by over ten times. In this technological wave, ionic materials have gained recognition as the most advanced adsorbents, demonstrating high efficacy in screening procedures applied to simulated nuclear waste.

Even with these significant strides, the field is still fraught with considerable challenges. For instance, a common issue faced by most inorganic adsorbents and all nano-based or nanostructured materials is the practicality of their deployment. The hindrance in actual nuclear waste studies is not due to a lack of interest, but instead, the difficulty in efficiently deploying loose powders under operative environmental conditions. While attaching them to a solid support like a monomer or a polymer seems intuitive, the additional weight of the substrate and the potential obstruction of the surface area may greatly compromise overall sorption capacity. This area remains minimally investigated, and until an approach is developed that only adds minimal mass without significant hindrance to surface area, the creation of new nanostructured materials might only remain an academic curiosity with limited practical significance. As such, rather than heavily focusing on the development of new materials, it is suggested that more efforts should be directed toward designing efficient deployment platforms. Furthermore, although advanced porous materials demonstrate superior adsorption capabilities compared to conventional materials, there is a need for continued research to develop scalable production methods and to lower the production costs for their widespread application.

Lastly, despite the substantial research dedicated to studying TcO<sub>4</sub><sup>-</sup> uptake under various conditions, there is a pressing need for further validation of the promising results found in existing literature, as well as for ensuring a more effective comparison between different studies. A thorough examination of the experimental conditions in numerous studies reveals significant

shortcomings that limit their applicability to real-world scenarios. Issues such as inappropriate pH levels, imbalanced phase ratios, unrealistic  $\text{TcO}_4^-$  concentrations, and the inclusion of irrelevant competing ions are some of the critical flaws that undermine the practical value of many published reports. The recent initiative to establish facilities for testing samples in environmental seawater is a commendable step toward addressing these issues, and there should be an emphasis on making these resources available to academic institutions. A major challenge that persists across all materials is their limited selectivity, particularly the difficulty in distinguishing between  $\text{TcO}_4^-$  and other commonly found anions in seawater like  $\text{SO}_4^{2-}$ ,  $\text{NO}_3^-$ , and  $\text{OH}^-$ . While many adsorbents show proficiency in extracting a significant portion of  $\text{TcO}_4^-$  from water samples, the research often falls short in demonstrating their effectiveness in selectively adsorbing  $\text{TcO}_4^-$  over these other ions. Additionally, verifying the long-term stability of advanced porous materials at officially designated nuclear waste sites is crucial. Sorbents that demonstrate stability in both strongly acidic and basic conditions are prioritized for practical applications.<sup>110</sup> Despite these challenges, there is optimism in the scientific community. Through the combined efforts of chemists, materials scientists, nuclear physicists, and chemical engineers, these obstacles can be effectively tackled. It is through this interdisciplinary collaboration that innovative solutions and advancements in the field of  $\text{TcO}_4^-$  extraction can be realized, ultimately contributing to safer and more efficient management of nuclear waste and environmental remediation.

## ■ ASSOCIATED CONTENT

### SI Supporting Information

The Supporting Information is available free of charge at <https://pubs.acs.org/doi/10.1021/cbe.3c00125>.

Comparative tables detailing the properties of  $\text{ReO}_4^-$  and  $\text{TcO}_4^-$ , alongside a performance analysis of adsorption capabilities between conventional materials and advanced porous materials for both  $\text{ReO}_4^-$  and  $\text{TcO}_4^-$  (PDF)

## ■ AUTHOR INFORMATION

### Corresponding Authors

**Qi Sun** – Zhejiang Provincial Key Laboratory of Advanced Chemical Engineering Manufacture Technology, College of Chemical and Biological Engineering, Zhejiang University, Hangzhou 310027, China; [orcid.org/0000-0002-1698-8741](https://orcid.org/0000-0002-1698-8741); Email: [sunqichs@zju.edu.cn](mailto:sunqichs@zju.edu.cn)

**Shengqian Ma** – Department of Chemistry, University of North Texas, Denton, Texas 76201, United States; [orcid.org/0000-0002-1897-7069](https://orcid.org/0000-0002-1897-7069); Email: [shengqian.ma@unt.edu](mailto:shengqian.ma@unt.edu)

### Authors

**Zhiwei Xing** – Zhejiang Provincial Key Laboratory of Advanced Chemical Engineering Manufacture Technology, College of Chemical and Biological Engineering, Zhejiang University, Hangzhou 310027, China; Present Address: College of Chemical Engineering, Nanjing Tech University, 30 South Puzhu Road, Nanjing 211816, China

**Zhuozhi Lai** – Zhejiang Provincial Key Laboratory of Advanced Chemical Engineering Manufacture Technology, College of Chemical and Biological Engineering, Zhejiang University, Hangzhou 310027, China

**Chengliang Xiao** – Zhejiang Provincial Key Laboratory of Advanced Chemical Engineering Manufacture Technology,

College of Chemical and Biological Engineering, Zhejiang University, Hangzhou 310027, China; [orcid.org/0000-0001-5081-2398](https://orcid.org/0000-0001-5081-2398)

**Shuao Wang** – State Key Laboratory of Radiation Medicine and Protection, School for Radiological and Interdisciplinary Sciences (RAD-X) and Collaborative Innovation Center of Radiation Medicine of Jiangsu Higher Education Institutions, Soochow University, Suzhou 215123, China; [orcid.org/0000-0002-1526-1102](https://orcid.org/0000-0002-1526-1102)

**Xiangke Wang** – MOE Key Laboratory of Resources and Environmental System Optimization, College of Environmental Science and Engineering, North China Electric Power University, Beijing 102206, PR China; [orcid.org/0000-0002-3352-1617](https://orcid.org/0000-0002-3352-1617)

**Briana Aguila-Ames** – New College of Florida, Sarasota, Florida 34343, United States

**Praveen K. Thallapally** – Physical and Computational Science Directorate, Pacific Northwest National Laboratory Richland, Richland, Washington 99352, United States; [orcid.org/0000-0001-7814-4467](https://orcid.org/0000-0001-7814-4467)

**Kyle Martin** – Department of Chemistry, University of North Texas, Denton, Texas 76201, United States

Complete contact information is available at: <https://pubs.acs.org/10.1021/cbe.3c00125>

## Author Contributions

<sup>¶</sup>The manuscript was written through contributions of all authors. All authors have given approval to the final version of the manuscript. Z.X. and Z.L. contributed equally.

## Notes

The authors declare no competing financial interest.

## ■ ACKNOWLEDGMENTS

This work was supported by the National Key Research and Development Program of China (2022YFA1503004), the Natural Science Foundation of Zhejiang province (LR23B060001 and LY22B06004), and the Robert A. Welch Foundation (B-0027).

## ■ REFERENCES

- (1) Bilgen, S. Structure and Environmental Impact of Global Energy Consumption. *Renew. Sust. Energy Rev.* **2014**, *38*, 890–902.
- (2) Maher, K.; Bargar, J. R.; Brown, G. E., Jr Environmental Speciation of Actinides. *Inorg. Chem.* **2013**, *52*, 3510–3532.
- (3) Lee, S.; Yoon, B.; Shin, J. Effects of Nuclear Energy on Sustainable Development and Energy Security: Sodium-Cooled Fast Reactor Case. *Sustain.* **2016**, *8*, 979.
- (4) Wang, Q.; Zhang, H.; Zhu, P. Using Nuclear Energy for Maritime Decarbonization and Related Environmental Challenges: Existing Regulatory Shortcomings and Improvements. *Int. J. Environ. Res. Public Health* **2023**, *20*, 2993.
- (5) Di, Z.; Mao, Y.; Yuan, H.; Zhou, Y.; Jin, J.; Li, C.-P. Covalent Organic Frameworks(COFs) for Sequestration of  $^{99}\text{TcO}_4^-$ . *Chem. Res. Chin Univ.* **2022**, *38*, 290–295.
- (6) Ahearn, J. F. Prospects for Nuclear Energy. *Energy Econ.* **2011**, *33*, 572–580.
- (7) Dittmar, M. Nuclear Energy: Status and Future Limitations. *Energy* **2012**, *37*, 35–40.
- (8) Sun, Y.; Wang, S.; Li, Y.; Lu, H.; Zhu, M.; Liu, X.; Chen, Z. Covalent Organic Frameworks (COF) Materials for Selective Radionuclides Removal from Water. *J. Radioanal. Nucl. Chem.* **2023**, *332*, 1101–1111.
- (9) Wang, X.; Chen, L.; Wang, L.; Fan, Q.; Pan, D.; Li, J.; Chi, F.; Xie, Y.; Yu, S.; Xiao, C.; Luo, F.; Wang, J.; Wang, X.; Chen, C.; Wu, W.; Shi,

- W.; Wang, S.; Wang, X. Synthesis of Novel Nanomaterials and Their Application in Efficient Removal of Radionuclides. *Sci. China Chem.* **2019**, *62*, 933–967.
- (10) Xiao, C.; Khayambashi, A.; Wang, S. Separation and Remediation of  $^{99}\text{TcO}_4^-$  from Aqueous Solutions. *Chem. Mater.* **2019**, *31*, 3863–3877.
- (11) Sadiq, M.; Shinwari, R.; Usman, M.; Ozturk, I.; Maghyereh, A. I. Linking Nuclear Energy, Human Development and Carbon Emission in BRICS region: Do External Debt and Financial Globalization Protect the Environment? *Nucl. Eng. Technol.* **2022**, *54*, 3299–3309.
- (12) Drace, Z.; Ojovan, M. I.; Samanta, S. K. Challenges in Planning of Integrated Nuclear Waste Management. *Sustain.* **2022**, *14*, 14204.
- (13) Zhi, X.; Li, X.; Dong, F.; Huang, Y.; Yang, S.; Yan, T.; Shen, Y. A Hydrophobic Imidazolium Cationic Framework for Selective Adsorption of  $\text{TcO}_4^-/\text{ReO}_4^-$  from Aqueous Solutions. *Mater. Adv.* **2022**, *3*, 4870–4877.
- (14) Li, C.-P.; Ai, J.-Y.; Zhou, H.; Chen, Q.; Yang, Y.; He, H.; Du, M. Ultra-Highly Selective Trapping of Perrhenate/Per technetate by a Flexible Cationic Coordination Framework. *Chem. Commun.* **2019**, *55*, 1841.
- (15) Fu, L.; Zu, J.; He, L.; Gu, E.; Wang, H. An Adsorption Study of  $^{99}\text{Tc}$  Using Nanoscale Zero-Valent Iron Supported on D001 Resin. *Front. Energy* **2020**, *14*, 11–17.
- (16) Fu, L.; Pan, X.; Zu, J.; He, L. Synthesis of Diamide-Based Resin for Selective Separation of  $^{99}\text{Tc}$ . *J. Radioanal. Nucl. Chem.* **2021**, *328*, 481–490.
- (17) Smith, F. N.; Taylor, C. D.; Um, W.; Kruger, A. A. Technetium Incorporation into Goethite ( $\alpha\text{-FeOOH}$ ): an Atomic-Scale Investigation. *Environ. Sci. Technol.* **2015**, *49*, 13699–13707.
- (18) Makarov, A. V.; Safonov, A. V.; Konevnik, Y. V.; Teterin, Y. A.; Maslakov, K. I.; Teterin, A. Y.; Karaseva, Y. Y.; German, K. E.; Zakharova, E. V. Activated Carbon Additives for Technetium Immobilization in Bentonite-Based Engineered Barriers for Radioactive Waste Repositories. *J. Hazard. Mater.* **2021**, *401*, 123436.
- (19) Shi, K.; Hou, X.; Roos, P.; Wu, W. Determination of Technetium-99 in Environmental Samples: a Review. *Anal. Chim. Acta* **2012**, *709*, 1–20.
- (20) Hu, Q.-H.; Weng, J.-Q.; Wang, J.-S. Sources of Anthropogenic Radionuclides in the Environment: a Review. *J. Environ. Radioact.* **2010**, *101*, 426–437.
- (21) Icenhower, J. P.; Qafoku, N. P.; Zachara, J. M.; Martin, W. J. The Biogeochemistry of Technetium: a Review Of the Behavior of an Artificial Element in the Natural Environment. *Am. J. Sci.* **2010**, *310*, 721–752.
- (22) Singh, B. K.; Mahzan, N. S.; Abdul Rashid, N. S.; Isa, S. A.; Hafeez, M. A.; Saslow, S.; Wang, G.; Mo, C.; Um, W. Design and Application of Materials for Sequestration and Immobilization of  $^{99}\text{Tc}$ . *Environ. Sci. Technol.* **2023**, *57*, 6776–6798.
- (23) Banerjee, D.; Kim, D.; Schweiger, M. J.; Kruger, A. A.; Thallapally, P. K. Removal of  $\text{TcO}_4^-$  Ions From Solution: Materials and Future Outlook. *Chem. Soc. Rev.* **2016**, *45*, 2724.
- (24) Liu, F.; Zheng, W.-F.; Zhang, Y.; Wang, H.; Zhou, C.-X. The Behavior of Technetium in Technetium-Scrubbing Stage of PUREX Process. *J. Radioanal. Nucl. Chem.* **2013**, *295*, 1621–1625.
- (25) Liu, F.; Sun, Y.-R.; Wang, H.; Zheng, W.-F. An Improved PUREX Process in Technetium Separation by Stepwise Reduction. *J. Radioanal. Nucl. Chem.* **2014**, *299*, 1329–1333.
- (26) Li, J.; Wang, X.; Zhao, G.; Chen, C.; Chai, Z.; Alsaedi, A.; Hayat, T.; Wang, X. Metal-Organic Framework-Based Materials: Superior Adsorbents for the Capture of Toxic and Radioactive Metal Ions. *Chem. Soc. Rev.* **2018**, *47*, 2322.
- (27) Zhu, L.; Xiao, C.; Dai, X.; Li, J.; Gui, D.; Sheng, D.; Chen, L.; Zhou, R.; Chai, Z.; Albrecht-Schmitt, T. E.; Wang, S. Exceptional Perrhenate/Per technetate Uptake and Subsequent Immobilization by a Low-Dimensional Cationic Coordination Polymer: Overcoming the Hofmeister Bias Selectivity. *Environ. Sci. Technol. Lett.* **2017**, *4*, 316–322.
- (28) Samanta, P.; Chandra, P.; Dutta, S.; Desai, A. V.; Ghosh, S. K. Chemically Stable Ionic Viologen-Organic Network: an Efficient Scavenger of Toxic Oxo-Anions from Water. *Chem. Sci.* **2018**, *9*, 7874.
- (29) Li, J.; Zhu, L.; Xiao, C.; Chen, L.; Chai, Z.; Wang, S. Efficient Uptake of Perrhenate/Per technetate from Aqueous Solutions by the Bifunctional Anion-Exchange Resin. *Radiochim. Acta* **2018**, *106*, 581–591.
- (30) King, W. D.; Hassan, N. M.; McCabe, D. J.; Hamm, L. L.; Johnson, M. E. Technetium Removal from Hanford and Savannah River Site Actual Tank Waste Supernates with Superlig<sup>®</sup>639 Resin. *Sep. Sci. Technol.* **2003**, *38*, 3093–3114.
- (31) Sarri, S.; Misaelides, P.; Zamboulis, D.; Gaona, X.; Altmaier, M.; Geckeis, H. Rhenium(VII) and Technetium(VII) Separation from Aqueous Solutions Using a Polyethylenimine-Epichlorohydrin Resin. *J. Radioanal. Nucl. Chem.* **2016**, *307*, 681–689.
- (32) Kang, M. J.; Rhee, S. W.; Moon, H. Sorption of  $\text{MO}_4^-$  ( $\text{M}=\text{Tc}$ ,  $\text{Re}$ ) on Mg/Al Layered Double Hydroxide by Anion Exchange. *Radiochim. Acta* **1996**, *75*, 169–173.
- (33) Kang, M. J.; Chun, K. S.; Rhee, S. W.; Do, Y. Comparison of Sorption Behavior of  $\text{I}^-$  and  $\text{TcO}_4^-$  on Mg/Al Layered Double Hydroxide. *Radiochim. Acta* **1999**, *85*, 57–63.
- (34) Wall, N. A.; Minai, Y. Adsorption of  $^{99}\text{TcO}_4^-$  onto Hydrotalcite and Calcined Hydrotalcite under Basic Conditions: Influence of Humic Acids and Anions. *J. Radioanal. Nucl. Chem.* **2014**, *301*, 221–225.
- (35) Daniels, N.; Franzen, C.; Murphy, G. L.; Kvashnina, K.; Petrov, V.; Torapava, N.; Bukaemskiy, A.; Kowalski, P.; Si, H.; Ji, Y.; Hölzer, A.; Walther, C. Application of Layered Double Hydroxides for  $^{99}\text{Tc}$  Remediation. *Appl. Clay Sci.* **2019**, *176*, 1–10.
- (36) Mayordomo, N.; Rodriguez, D.M.; Rossberg, A.; Foerstendorf, H.; Heim, K.; Brendler, V.; Muller, K. Analysis of Technetium Immobilization and Its Molecular Retention Mechanisms by Fe(II)-Al(III)-Cl Layered Double Hydroxide. *Chem. Eng. J.* **2021**, *408*, 127265.
- (37) Li, D.; Kaplan, D. I.; Knox, A. S.; Crapse, K. P.; Diprete, D. P. Aqueous  $^{99}\text{Tc}$ ,  $^{129}\text{I}$  and  $^{137}\text{Cs}$  Removal from Contaminated Groundwater and Sediments Using Highly Effective Low-Cost Sorbents. *J. Environ. Radioact.* **2014**, *136*, 56–63.
- (38) Milutinović-Nikolić, A.; Maksin, D.; Jović-Jovičić, N.; Mirković, M.; Stanković, D.; Mojović, Z.; Banković, P. Removal of  $^{99}\text{Tc(VII)}$  by Organo-Modified Bentonite. *Appl. Clay Sci.* **2014**, *95*, 294–302.
- (39) Luo, W.; Inoue, A.; Hirajima, T.; Sasaki, K. Synergistic Effect of  $\text{Sr}^{2+}$  and  $\text{ReO}_4^-$  Adsorption on Hexadecyl Pyridinium-Modified Montmorillonite. *Appl. Surf. Sci.* **2017**, *394*, 431–439.
- (40) Xiong, Y.; Cui, X.; Zhang, P.; Wang, Y.; Lou, Z.; Shan, W. Improving Re(VII) Adsorption on Diisobutylamine-Functionalized Graphene Oxide. *ACS Sustain. Chem. Eng.* **2017**, *5*, 1010–1018.
- (41) Zhang, H.; Yang, F.; Lu, C.; Du, C.; Bai, R.; Zeng, X.; Zhao, Z.; Cai, C.; Li, J. Effective Decontamination of  $^{99}\text{TcO}_4^-/\text{ReO}_4^-$  from Hanford Low-Activity Waste by Functionalized Graphene Oxide-Chitosan Sponges. *Environ. Chem. Lett.* **2020**, *18*, 1379–1388.
- (42) Wang, K.; Yan, Z.; Fu, L.; Li, D.; Gong, L.; Wang, Y.; Xiong, Y. Gemini Ionic Liquid Modified Nacre-Like Reduced Graphene Oxide Click Membranes for  $\text{ReO}_4^-/\text{TcO}_4^-$  Removal. *Sep. Purif. Technol.* **2022**, *302*, 122073.
- (43) Furukawa, H.; Cordova, K. E.; O’Keeffe, M.; Yaghi, O. M. The Chemistry and Applications of Metal-Organic Frameworks. *Science* **2013**, *341*, 1230444.
- (44) Li, J.-R.; Kuppler, R. J.; Zhou, H.-C. Selective Gas Adsorption and Separation in Metal-Organic Frameworks. *Chem. Soc. Rev.* **2009**, *38*, 1477–1504.
- (45) Schneemann, A.; Bon, V.; Schwedler, I.; Senkovska, I.; Kaskel, S.; Fischer, R. A. Flexible Metal-Organic Frameworks. *Chem. Soc. Rev.* **2014**, *43*, 6062–6096.
- (46) Ding, M.; Flaig, R. W.; Jiang, H.-L.; Yaghi, O. M. Carbon Capture and Conversion Using Metal-Organic Frameworks and MOF-Based Materials. *Chem. Soc. Rev.* **2019**, *48*, 2783–2828.
- (47) Howarth, A. J.; Liu, Y.; Li, P.; Li, Z.; Wang, T. C.; Hupp, J. T.; Farha, O. K. Chemical, Thermal and Mechanical Stabilities of Metal-Organic Frameworks. *Nat. Rev. Mater.* **2016**, *1*, 15018.

- (48) Diercks, C. S.; Yaghi, O. M. The Atom, the Molecule, and the Covalent Organic Framework. *Science* **2017**, *355*, 1585.
- (49) Ding, S.-Y.; Wang, W. Covalent Organic Frameworks (COFs): From Design to Applications. *Chem. Soc. Rev.* **2013**, *42*, 548–568.
- (50) Liu, X.; Huang, D.; Lai, C.; Zeng, G.; Qin, L.; Wang, H.; Yi, H.; Li, B.; Liu, S.; Zhang, M.; Deng, R.; Fu, Y.; Li, L.; Xue, W.; Chen, S. Recent Advances in Covalent Organic Frameworks (COFs) as a Smart Sensing Material. *Chem. Soc. Rev.* **2019**, *48*, 5266–5302.
- (51) Liu, Y.; Zhou, W.; Teo, W.; Wang, K.; Zhang, L.; Zeng, Y.; Zhao, Y. Covalent-Organic-Framework-Based Composite Materials. *Chem.* **2020**, *6*, 3172–3202.
- (52) Liu, X.; Pang, H.; Liu, X.; Li, Q.; Zhang, N.; Mao, L.; Qiu, M.; Hu, B.; Yang, H.; Wang, X. Orderly Porous Covalent Organic Frameworks-Based Materials: Superior Adsorbents for Pollutants Removal from Aqueous Solutions. *Innovation* **2021**, *2*, 100076.
- (53) Singh, G.; Lee, J.; Karakoti, A.; Bahadur, R.; Yi, J.; Zhao, D.; AlBahily, K.; Vinu, A. Emerging Trends in Porous Materials for CO<sub>2</sub> Capture and Conversion. *Chem. Soc. Rev.* **2020**, *49*, 4360–4404.
- (54) Zou, L.; Sun, Y.; Che, S.; Yang, X.; Wang, X.; Bosch, M.; Wang, Q.; Li, H.; Smith, M.; Yuan, S.; Perry, Z.; Zhou, H.-C. Porous Organic Polymers for Post-Combustion Carbon Capture. *Adv. Mater.* **2017**, *29*, 1700229.
- (55) Ji, W.; Wang, T.-X.; Ding, X.; Lei, S.; Han, B.-H. Porphyrin- and Phthalocyanine-Based Porous Organic Polymers: from Synthesis to Application. *Coord. Chem. Rev.* **2021**, *439*, 213875.
- (56) Banerjee, D.; Xu, W.; Nie, Z.; Johnson, L. E. V.; Coghlan, C.; Sushko, M. L.; Kim, D.; Schweiger, M. J.; Kruger, A. A.; Doonan, C. J.; Thallapally, P. K. Zirconium-Based Metal-Organic Framework for Removal of Perrhenate from Water. *Inorg. Chem.* **2016**, *55*, 8241–8243.
- (57) Zhong, X.; Liang, W.; Wang, H.; Xue, C.; Hu, B. Aluminum-Based Metal-Organic Frameworks (CAU-1) Highly Efficient UO<sub>2</sub><sup>2+</sup> and TcO<sub>4</sub><sup>-</sup> Ions Immobilization from Aqueous Solution. *J. Hazard. Mater.* **2021**, *407*, 124729.
- (58) Sheng, D.; Zhu, L.; Xu, C.; Xiao, C.; Wang, Y.; Wang, Y.; Chen, L.; Diwu, J.; Chen, J.; Chai, Z.; Albrecht-Schmitt, T. E.; Wang, S. Efficient and Selective Uptake of TcO<sub>4</sub><sup>-</sup> by a Cationic Metal-Organic Framework Material with Open Ag<sup>+</sup> Sites. *Environ. Sci. Technol.* **2017**, *51*, 3471–3479.
- (59) Zhu, L.; Sheng, D.; Xu, C.; Dai, X.; Silver, M. A.; Li, J.; Li, P.; Wang, Y.; Wang, Y.; Chen, L.; Xiao, C.; Chen, J.; Zhou, R.; Zhang, C.; Farha, O. K.; Chai, Z.; Albrecht-Schmitt, T. E.; Wang, S. Identifying the Recognition Site for Selective Trapping of <sup>99</sup>TcO<sub>4</sub><sup>-</sup> in a Hydrolytically Stable and Radiation Resistant Cationic Metal-Organic Framework. *J. Am. Chem. Soc.* **2017**, *139*, 14873–14876.
- (60) Sheng, D.; Zhu, L.; Dai, X.; Xu, C.; Li, P.; Pearce, C. I.; Xiao, C.; Chen, J.; Zhou, R.; Duan, T.; Farha, O. K.; Chai, Z.; Wang, S. Successful Decontamination of <sup>99</sup>TcO<sub>4</sub><sup>-</sup> in Groundwater at Legacy Nuclear Sites by a Cationic Metal-Organic Framework with Hydrophobic Pockets. *Angew. Chem. Int. Ed.* **2019**, *58*, 4968–4972.
- (61) Drout, R. J.; Otake, K.; Howarth, A. J.; Islamoglu, T.; Zhu, L.; Xiao, C.; Wang, S.; Farha, O. K. Efficient Capture of Perrhenate and Per technetate by a Mesoporous Zr Metal-Organic Framework and Examination of Anion Binding Motifs. *Chem. Mater.* **2018**, *30*, 1277–1284.
- (62) Li, D.; Shustova, N. B.; Martin, C. R.; Taylor-Pashow, K.; Seaman, J. C.; Kaplan, D. I.; Amoroso, J. W.; Chernikov, R. Anion-Exchanged and Quaternary Ammonium Functionalized MIL-101-Cr Metal-Organic Framework (MOF) for ReO<sub>4</sub><sup>-</sup>/TcO<sub>4</sub><sup>-</sup> Sequestration from Groundwater. *J. Environ. Radioactiv.* **2020**, *222*, 106372.
- (63) Ma, J.; Wang, C.-C.; Zhao, Z.-X.; Wang, P.; Li, J.-J.; Wang, F.-X. Adsorptive Capture of Perrhenate (ReO<sub>4</sub><sup>-</sup>) from Simulated Wastewater by Cationic 2D-MOF BUC-17. *Polyhedron* **2021**, *202*, 115218.
- (64) Kang, K.; Li, L.; Zhang, M.; Zhang, X.; Lei, L.; Xiao, C. Constructing Cationic Metal-Organic Framework Materials Based on Pyrimidyl as a Functional Group for Perrhenate/Per technetate Sorption. *Inorg. Chem.* **2021**, *60*, 16420–16428.
- (65) Kang, K.; Shen, N.; Wang, Y.; Li, L.; Zhang, M.; Zhang, X.; Lei, L.; Miao, X.; Wang, S.; Xiao, C. Efficient Sequestration of Radioactive <sup>99</sup>TcO<sub>4</sub><sup>-</sup> by a Rare 3-fold Interlocking Cationic Metal-Organic Framework: a Combined Batch Experiments, Pair Distribution Function, and Crystallographic Investigation. *Chem. Eng. J.* **2022**, *427*, 130942.
- (66) Kang, K.; Li, L.; Zhang, M.; Miao, X.; Lei, L.; Xiao, C. Two-fold Interlocking Cationic Metal-Organic Framework Material with Exchangeable Chloride for Perrhenate/Per technetate Sorption. *Inorg. Chem.* **2022**, *61*, 11463–11470.
- (67) Feng, H.; Xiong, X.; Gong, L.; Zhang, H.; Xu, Y.; Feng, X.; Luo, F. Rational Tuning of Thorium-Organic Frameworks by Reticular Chemistry for Boosting Radionuclide Sequestration. *Nano Res.* **2022**, *15*, 1472–1478.
- (68) Rapti, S.; Diamantis, S. A.; Dafnomili, A.; Pournara, A.; Skliri, E.; Armatas, G. S.; Tspis, A. C.; Spanopoulos, I.; Malliakas, C. D.; Kanatzidis, M. G.; Plakatouras, J. C.; Noli, F.; Lazarides, T.; Manos, M. J. Exceptional TcO<sub>4</sub><sup>-</sup> Sorption Capacity and Highly Efficient ReO<sub>4</sub><sup>-</sup> Luminescence Sensing by Zr<sub>4</sub><sup>+</sup> MOFs. *J. Mater. Chem. A* **2018**, *6*, 20813–20821.
- (69) Deng, S.-Q.; Mo, X.-J.; Zheng, S.-R.; Jin, X.; Gao, Y.; Cai, S.-L.; Fan, J.; Zhang, W.-G. Hydrolytically Stable Nanotubular Cationic Metal-Organic Framework for Rapid and Efficient Removal of Toxic Oxo-Anions and Dyes from Water. *Inorg. Chem.* **2019**, *58*, 2899–2909.
- (70) Li, C.-P.; Li, H.-R.; Ai, J.-Y.; Chen, J.; Du, M. Optimizing Strategy for Enhancing the Stability and <sup>99</sup>TcO<sub>4</sub><sup>-</sup> Sequestration of Poly(ionic liquids)/MOFs Composites. *ACS Cent. Sci.* **2020**, *6*, 2354–2361.
- (71) Zhang, G.; Tan, K.; Xian, S.; Xing, K.; Sun, H.; Hall, G.; Li, L.; Li, J. Ultrastable Zirconium-Based Cationic Metal-Organic Frameworks for Perrhenate Removal from Wastewater. *Inorg. Chem.* **2021**, *60*, 11730–11738.
- (72) Shen, N.; Yang, Z.; Liu, S.; Dai, X.; Xiao, C.; Taylor-Pashow, K.; Li, D.; Yang, C.; Li, J.; Zhang, Y.; Zhang, M.; Zhou, R.; Chai, Z.; Wang, S. <sup>99</sup>TcO<sub>4</sub><sup>-</sup> Removal from Legacy Defense Nuclear Waste by an Alkaline-Stable 2D Cationic Metalorganic Framework. *Nat. Commun.* **2020**, *11*, 5571.
- (73) Kang, K.; Liu, S.; Zhang, M.; Li, L.; Liu, C.; Lei, L.; Dai, X.; Xu, C.; Xiao, C. Fast Room-Temperature Synthesis of an Extremely Alkaline-Resistant Cationic Metal-Organic Framework for Sequestering TcO<sub>4</sub><sup>-</sup> with Exceptional Selectivity. *Adv. Funct. Mater.* **2022**, *32*, 2208148.
- (74) Hu, Q.-H.; Shi, Y.-Z.; Gao, X.; Zhang, L.; Liang, R.-P.; Qiu, J.-D. An Alkali-Resistant Metal-Organic Framework as Halogen Bond Donor for Efficient and Selective Removing of ReO<sub>4</sub><sup>-</sup>/TcO<sub>4</sub><sup>-</sup>. *Environ. Sci. Pollut. R.* **2022**, *29*, 86815–86824.
- (75) Hu, Q.-H.; Wang, Y.-G.; Gao, X.; Shi, Y.-Z.; Lin, S.; Liang, R.-P.; Qiu, J.-D. Halogen Microregulation in Metal-Organic Frameworks for Enhanced Adsorption Performance of ReO<sub>4</sub><sup>-</sup>/TcO<sub>4</sub><sup>-</sup>. *J. Hazard. Mater.* **2023**, *446*, 130744.
- (76) Hu, Q.-H.; Gao, X.; Shi, Y.-Z.; Liang, R.-P.; Zhang, L.; Lin, S.; Qiu, J.-D. Tailor-Made Multiple Interpenetrated Metal-Organic Framework for Selective Detection and Adsorption of ReO<sub>4</sub><sup>-</sup>. *Anal. Chem.* **2022**, *94*, 16864–16870.
- (77) Mollick, S.; Fajal, S.; Saurabh, S.; Mahato, D.; Ghosh, S. K. Nanotrap Grafted Anion Exchangeable Hybrid Materials for Efficient Removal of Toxic Oxoanions from Water. *ACS Cent. Sci.* **2020**, *6*, 1534–1541.
- (78) Wang, Y.; Xie, M.; Lan, J.; Yuan, L.; Yu, J.; Li, J.; Peng, J.; Chai, Z.; Gibson, J. K.; Zhai, M.; Shi, W. Radiation Controllable Synthesis of Robust Covalent Organic Framework Conjugates for Efficient Dynamic Column Extraction of <sup>99</sup>TcO<sub>4</sub><sup>-</sup>. *Chem.* **2020**, *6*, 2796–2809.
- (79) Wang, Y.; Lan, J.; Yang, X.; Zhong, S.; Yuan, L.; Li, J.; Peng, J.; Chai, Z.; Gibson, J. K.; Zhai, M.; Shi, W. Superhydrophobic Phosphonium Modified Robust 3D Covalent Organic Framework for Preferential Trapping of Charge Dispersed Oxoanionic Pollutants. *Adv. Funct. Mater.* **2022**, *32*, 2205222.
- (80) Da, H.-J.; Yang, C.-X.; Yan, X.-Y. Cationic Covalent Organic Nanosheets for Rapid and Selective Capture of Perrhenate: an Analogue of Radioactive Per technetate from Aqueous Solution. *Environ. Sci. Technol.* **2019**, *53*, 5212–5220.
- (81) Zhao, P.; Zhou, X.; Huang, Y.; Xu, Y.; Chen, S.; Zheng, C.; Jin, Y.; Xia, C. Cationic Covalent Organic Polymers Based on Guanidine with

Higher Positive Potential for Selective Sorption of  $\text{ReO}_4^-$ : Synthesis and DFT Calculation. *Surf. Interfaces* **2022**, *29*, 101788.

(82) He, L.; Liu, S.; Chen, L.; Dai, X.; Li, J.; Zhang, M.; Ma, F.; Zhang, C.; Yang, Z.; Zhou, R.; Chai, Z.; Wang, S. Mechanism Unravelling for Ultrafast and Selective  $^{99}\text{TcO}_4^-$  Uptake by a Radiation-Resistant Cationic Covalent Organic Framework: a Combined Radiological Experiment and Molecular Dynamics Simulation Study. *Chem. Sci.* **2019**, *10*, 4293–4305.

(83) Chen, X.-R.; Zhang, C.-R.; Jiang, W.; Liu, X.; Luo, Q.-X.; Zhang, L.; Liang, R.-P.; Qiu, J.-D. 3D Viologen-Based Covalent Organic Framework for Selective and Efficient Adsorption of  $\text{ReO}_4^-/\text{TcO}_4^-$ . *Sep. Purif. Technol.* **2023**, *312*, 123409.

(84) Hao, M.; Chen, Z.; Yang, H.; Waterhouse, G. I. N.; Ma, S.; Wang, X. Pyridinium Salt-Based Covalent Organic Framework with Well-Defined Nanochannels for Efficient and Selective Capture of Aqueous  $^{99}\text{TcO}_4^-$ . *Sci. Bull.* **2022**, *67*, 924–932.

(85) Liu, Z.-F.; Liu, K.; Zheng, X.-J.; Wang, Y.-H.; Sun, X.-X.; Xue, P.-C.; Li, C.-P.; Du, M. Formulation of Poly(ionic liquids)@COF Nanotrap for Efficient Perrhenate Sequestration from Alkaline Nuclear Waste. *Chem. Mater.* **2022**, *34*, 5452–5460.

(86) Cui, W.-R.; Xu, W.; Chen, Y.-R.; Liu, K.; Qiu, W.-B.; Li, Y.; Qiu, J.-D. Olefin-Linked Cationic Covalent Organic Frameworks for Efficient Extraction of  $\text{ReO}_4^-/^{99}\text{TcO}_4^-$ . *J. Hazard. Mater.* **2023**, *446*, 130603.

(87) Zhang, C.-R.; Cui, W.-R.; Yi, S.-M.; Niu, C.-P.; Liang, R.-P.; Qi, J.-X.; Chen, X.-J.; Jiang, W.; Liu, X.; Luo, Q.-X.; Qiu, J.-D. An ionic Vinylene-Linked Three-Dimensional Covalent Organic Framework for Selective and Efficient Trapping of  $\text{ReO}_4^-$  or  $^{99}\text{TcO}_4^-$ . *Nat. Commun.* **2022**, *13*, 7621.

(88) Yi, S.-M.; Zhang, C.-R.; Jiang, W.; Liu, X.; Niu, C.-P.; Qi, J.-X.; Chen, X.-J.; Liang, R.-P.; Qiu, J.-D. Ionic Liquid Modified Covalent Organic Frameworks for Efficient Detection and Adsorption of  $\text{ReO}_4^-/\text{TcO}_4^-$ . *J. Environ. Chem. Eng.* **2022**, *10*, 107666.

(89) Li, J.; Dai, X.; Zhu, L.; Xu, C.; Zhang, D.; Silver, M. A.; Li, P.; Chen, L.; Li, Y.; Zuo, D.; Zhang, H.; Xiao, C.; Chen, J.; Diwu, J.; Farha, O. K.; Albrecht-Schmitt, T. E.; Chai, Z.; Wang, S.  $^{99}\text{TcO}_4^-$  Remediation by a Cationic Polymeric Network. *Nat. Commun.* **2018**, *9*, 3007.

(90) Sun, Q.; Zhu, L.; Aguila, B.; Thallapally, P. K.; Xu, C.; Chen, J.; Wang, S.; Rogers, D.; Ma, S. Optimizing Radionuclide Sequestration in Anion Nanotraps with Record Perchnetate Sorption. *Nat. Commun.* **2019**, *10*, 1646.

(91) Liu, Z.-W.; Han, B.-H. Evaluation of an Imidazolium-Based Porous Organic Polymer as Radioactive Waste Scavenger. *Environ. Sci. Technol.* **2020**, *54*, 216–224.

(92) Ding, M.; Chen, L.; Xu, Y.; Chen, B.; Ding, J.; Wu, R.; Huang, C.; He, Y.; Jin, Y.; Xia, C. Efficient Capture of Tc/Re(VI, IV) by a Viologen-Based Organic Polymer Containing Tetraaza Macrocycles. *Chem. Eng. J.* **2020**, *380*, 122581.

(93) Li, J.; Chen, L.; Shen, N.; Xie, R.; Sheridan, M. V.; Chen, X.; Sheng, D.; Zhang, D.; Chai, Z.; Wang, S. Rational Design of a Cationic Polymer Network Towards Record High Uptake of  $^{99}\text{TcO}_4^-$  in Nuclear Waste. *Sci. China Chem.* **2021**, *64*, 1251–1260.

(94) Li, X.; Li, Y.; Wang, H.; Niu, Z.; He, Y.; Jin, L.; Wu, M.; Wang, H.; Chai, L.; Al-Enizi, A. M.; Nafady, A.; Shaikh, S. F.; Ma, S. 3D Cationic Polymeric Network Nanotrap for Efficient Collection of Perrhenate Anion from Wastewater. *Small* **2021**, *17*, 2007994.

(95) Jiao, S.; Deng, L.; Zhang, X.; Zhang, Y.; Liu, K.; Li, S.; Wang, L.; Ma, D. Evaluation of an Ionic Porous Organic Polymer for Water Remediation. *ACS Appl. Mater. Interfaces* **2021**, *13*, 39404–39413.

(96) Huang, M.; Kan, L.; Zhao, W.; Wang, Y.; Xiong, Y.; Shan, W.; Lou, Z. Highly Efficient and Selective Capture of  $\text{TcO}_4^-$  or  $\text{ReO}_4^-$  by Imidazolium-Based Ionic Liquid Polymers. *Chem. Eng. J.* **2021**, *421*, 127763.

(97) Sen, A.; Dutta, S.; Dam, G. K.; Samanta, P.; Let, S.; Sharma, S.; Shirolkar, M. M.; Ghosh, S. K. Imidazolium-Functionalized Chemically Robust Ionic Porous Organic Polymers (iPOPs) Toward Toxic Oxo-Pollutants Capture from Water. *Chem.—Eur. J.* **2021**, *27*, 13442–13449.

(98) Hu, Q.-H.; Jiang, W.; Liang, R.-P.; Lin, S.; Qiu, J.-D. Synthesis of Imidazolium-Based Cationic Organic Polymer for Highly Efficient and Selective Removal of  $\text{ReO}_4^-/\text{TcO}_4^-$ . *Chem. Eng. J.* **2021**, *419*, 129546.

(99) Kang, K.; Zhang, M.; Li, L.; Lei, L.; Xiao, C. Selective Sequestration of Perrhenate by Cationic Polymeric Networks Based on Elongated Pyridyl Ligands. *Ind. Eng. Chem. Res.* **2022**, *61*, 18870–18880.

(100) Wu, W.; Liu, X.; Yang, X.; Xiao, Q.; Liu, Y.; Wang, S.; Wang, X.-F. Facile Synthesis of Imidazolium Cationic Organic Polymer with Ultrafast  $\text{ReO}_4^-/^{99}\text{TcO}_4^-$  Removal under Highly Alkaline Conditions. *Sep. Purif. Technol.* **2023**, *318*, 123951.

(101) Peng, H.; Jiang, B.; Li, F.; Gong, J.; Zhang, Y.; Yang, M.; Liu, N.; Ma, L. Single-Crystal-Structure Directed Predesign of Cationic Covalent Organic Polymers for Rapidly Capturing  $^{99}\text{TcO}_4^-$ . *Chem. Mater.* **2023**, *35*, 2531–2540.

(102) Qi, J.-X.; Zhang, C.-R.; Chen, X.-J.; Yi, S.-M.; Niu, C.-P.; Liu, J.-L.; Zhang, L.; Liang, R.-P.; Qiu, J.-D. 3D Ionic Olefin-Linked Conjugated Microporous Polymers for Selective Detection and Removal of  $\text{TcO}_4^-/\text{ReO}_4^-$  from Wastewater. *Anal. Chem.* **2022**, *94*, 10850–10856.

(103) Yan, R.-H.; Cui, W.-R.; Jiang, W.; Huang, J.; Liang, R.-P.; Qiu, J.-D. Rationally Designed Pyridinium Cationic Polymeric Network for Effective  $\text{TcO}_4^-/\text{ReO}_4^-$  Remediation. *Chem. Eng. J.* **2023**, *268*, 118403.

(104) Li, J.; Li, B.; Shen, N.; Chen, L.; Guo, Q.; Chen, L.; He, L.; Dai, X.; Chai, Z.; Wang, S. Task-Specific Tailored Cationic Polymeric Network with High Base Resistance for Unprecedented  $^{99}\text{TcO}_4^-$  Cleanup from Alkaline Nuclear Waste. *ACS Cent. Sci.* **2021**, *7*, 1441–1450.

(105) Yang, X.; Wu, W.; Xie, Y.; Hao, M.; Liu, X.; Chen, Z.; Yang, H.; Waterhouse, G. I. N.; Ma, S.; Wang, X. Modulating Anion Nanotraps Via Halogenation for High-Efficiency  $^{99}\text{TcO}_4^-/\text{ReO}_4^-$  Removal under Wide-ranging pH Conditions. *Environ. Sci. Technol.* **2023**, *57*, 10870–10881.

(106) Yi, S.-M.; Zhang, C.-R.; Liu, X.; Jiang, W.; Liang, R.-P.; Qiu, J.-D. Molecular Engineering of Cationic Polymer Networks for Enhanced  $^{99}\text{TcO}_4^-/\text{ReO}_4^-$  Removal Efficiency in Extreme Environments. *Mater. Chem. Phys.* **2023**, *306*, 128032.

(107) Wang, Y.-G.; Hu, Q.-H.; Huang, J.; Jiang, W.; Zhang, L.; Liang, R.-P.; Qiu, J.-D. Synthesis of Cationic Polymer Decorated with Halogen for Highly Efficient Trapping  $^{99}\text{TcO}_4^-/\text{ReO}_4^-$ . *J. Hazard. Mater.* **2023**, *443*, 130325.

(108) Yuan, L.; Xu, R.; Yu, H.; Ji, C.; Lv, L.; Zhang, W. Three-Dimensional Fluorinated Pyrazinium-Based Cationic Organic Polymers with High Charge Density for Enhanced  $\text{ReO}_4^-$  Removal. *Chem. Eng. J.* **2023**, *475*, 146085.

(109) Xu, W.; Wang, X.; Li, Y.; Cui, W.-R. Ultra-Stable 3D Pyridinium Salt-Based Polymeric Network Nanotrap for Selective  $^{99}\text{TcO}_4^-/\text{ReO}_4^-$  Capture Via Hydrophobic and Steric Engineering. *J. Hazard. Mater.* **2023**, *455*, 131549.

(110) Wang, B.; Li, J.; Huang, H.; Liang, B.; Zhang, Y.; Chen, L.; Tan, K.; Chai, Z.; Wang, S.; Wright, J. T.; Meulenberg, R. W.; Ma, S. Creation of Cationic Polymeric Nanotrap Featuring High Anion Density and Exceptional Alkaline Stability for Highly Efficient Perchnetate Removal from Nuclear Waste Streams. *ACS Cent. Sci.* **2024**, DOI: 10.1021/acscentsci.3c01323.

## NOTE ADDED AFTER ASAP PUBLICATION

This paper was published ASAP on February 22, 2024, with an error in the TOC/Abstract. The corrected version was reposted February 26, 2024.